arXiv:cond-mat/9309006v1 8 Sep 1993

Charge and Spin Gap Formation in Exactly Solvable Hubbard Chains with Long-Range Hopping

Florian Gebhard and Andreas Girndt

Dept. of Physics and Materials Sciences Center, Philipps University, D-35032 Marburg, Germany

Andrei E. Ruckenstein

Serin Physics Laboratory, Rutgers University, P.O. Box 849, Piscataway, NJ 08855-0849

(February 6, 2008)

Abstract

We discuss the transition from a metal to charge or spin insulating phases characterized by the opening of a gap in the charge or spin excitation spectra, respectively. These transitions are addressed within the context of two exactly solvable Hubbard and tJ chains with long range, $1/r$ hopping. We discuss the specific heat, compressibility, and magnetic susceptibility of these models as a function of temperature, band filling, and interaction strength. We then use conformal field theory techniques to extract ground state correlation functions. Finally, by employing the g-ology analysis we show that the charge insulator transition is accompanied by an infinite discontinuity in the Drude weight of the electrical conductivity. While the magnetic properties of these models reflect the genuine features of strongly correlated electron systems, the charge transport properties, especially near the Mott-Hubbard transition, display a non-generic behavior.

PACS1993: 71.27.+a, 71.30.+h, 05.30.Fk

Typeset using REVTEX

I. INTRODUCTION

Recently[1] we introduced a Hubbard-like model which describes spin-1/2 Fermions on a chain of L sites, hopping with long-range amplitude, $t_{l,m} = it(-1)^{l-m}\left[d(l-m)\right]^{-1}$. Here, $d(l-m) = (L/\pi)\sin[\pi(l-m)/L]$ is the chord distance between sites l and m on the chain closed into a ring (the lattice spacing a is set to unity). In the thermodynamic limit, $L \to \infty$, and for a fixed distance, $(l-m)$, the purely imaginary hopping $t_{l,m} = t^*_{m,l}$ becomes $t_{l,m} \to it/(l-m)$, leading to the Hubbard Hamiltonian with "$1/r$-hopping",

$$\hat{H} = \hat{T} + U\hat{D} = \sum_{l\neq m=1,\sigma}^{L} t_{l,m}\hat{c}^{+}_{l,\sigma}\hat{c}_{m,\sigma} + U\sum_{l=1}^{L}\hat{n}_{l,\uparrow}\hat{n}_{l,\downarrow} \quad . \tag{1}$$

Here U is the strength of the usual local Hubbard[2] interaction. For even L we choose antiperiodic boundary conditions, so that the dispersion relation is linear in wave vector, namely, $\epsilon(k) = tk$ for $k = \Delta(m+1/2)$ ($\Delta = 2\pi/L$, $m = -L/2, \dots, L/2-1$). For $U = 0$ the Fermi sea is the ground state with all k-states from $k = -\pi$ to $k_F^e = \pi(n-1)$ filled[3], where $n = (N_\uparrow + N_\downarrow)/L$ is the total particle density (the "filling"). Note that the kinetic and potential energy operators are respectively odd and even under partity, and thus parity is, in general, not a good quantum number in our model.

In the large U limit the Hamiltonian (1) becomes the $1/r$-tJ model including "pair-hopping" terms ($\hat{P}_{D=0}$ projects onto the subspace with no double occupancies)[4]:

$$\begin{aligned}\hat{H}_{\text{tJ}} = \hat{P}_{D=0}\Big\{\hat{T} + \sum_{l\neq m}\frac{2|t_{l,m}|^2}{U}\left[\hat{\mathbf{S}}_l\cdot\hat{\mathbf{S}}_m - \frac{1}{4}\hat{n}_l\hat{n}_m\right] \\ - \sum_{l\neq n\neq m\neq l}\frac{t_{l,n}t_{n,m}}{U}\sum_{\sigma\sigma'}(\sigma\sigma')\,\hat{c}^{+}_{l\sigma}\hat{c}^{+}_{n-\sigma}\hat{c}_{n-\sigma'}\hat{c}_{m\sigma'}\Big\}\hat{P}_{D=0} \quad .\end{aligned} \tag{2}$$

As usual, $\hat{n}_l = \hat{n}_{l,\uparrow} + \hat{n}_{l,\downarrow}$, and $\hat{\mathbf{S}}_l$ is the spin-1/2 vector operator ($\hat{S}^+_l = \hat{c}^+_{l,\uparrow}\hat{c}_{l,\downarrow}$, $\hat{S}^-_l = \hat{c}^+_{l,\downarrow}\hat{c}_{l,\uparrow}$, $\hat{S}^z_l = (\hat{n}_{l,\uparrow} - \hat{n}_{l,\downarrow})/2$). At half filling, where the first and third terms in (2) vanish, the model (2) reduces to the (parity symmetric) $(1/r)^2$-Heisenberg model introduced by Haldane and Shastry[5], with $J = 4t^2/U$.

In Ref. 1 we conjectured the full excitation spectrum and associated degeneracies, and were thus able to calculate the free energy. The exact solution allowed us to identify two zero temperature ($T = 0$) phase transitions: the first was a Mott-Hubbard[2,6] metal-to-charge-insulator transition (MCIT) in the half-filled $1/r$-Hubbard model. This was signaled by the opening of a charge gap for $U > U_c = W$ where $W = 2\pi t$ is the electron bandwidth. The second, a metal-to-spin insulator transition (MSIT) was associated with the opening of a spin gap in the $1/r$-tJ model (2) for $J > J_c = 2W/\left[(1-n)\pi^2\right]$.

In this paper we clarify the nature of these transitions and attempt to separate the features due to the special form of the dispersion in (1) from more generic properties which may be expected to survive for other dispersions and/or in higher dimensions. The plan of the paper is as follows: we start in section II by recalling the form of our exact solution for the spectrum and ground state energies, from which we identify the location of the MCIT and MSIT. In section III we discuss the thermodynamic properties of our two models, namely the specific heat, compressibility, and magnetic susceptibility. In sec. IV we use conformal field theory techniques to extract the long-range behavior of ground state correlation functions. Sec. V contains a discussion of the connection with the "g-ology" approach to one-dimensional systems, which we exemplify by calculating the Drude weight in the frequency dependent electrical conductivity for the $1/r$-Hubbard model. Finally, a summary and conclusions are presented in sec. VI.

II. GROUND STATE PROPERTIES AND EXCITATION SPECTRA

We recall the effective Hamiltonian, introduced in ref. 1,

$$\hat{H}^{\rm eff} = \sum_{-\pi<\mathcal{K}<\pi} \left\{ \sum_{\sigma} h^s_{\mathcal{K},\sigma}\tilde{n}^s_{\mathcal{K},\sigma} + h^d_{\mathcal{K}}\tilde{n}^d_{\mathcal{K}} + h^e_{\mathcal{K}}\tilde{n}^e_{\mathcal{K}} + J_{\mathcal{K}}\left[\tilde{n}^d_{\mathcal{K}-\Delta}\tilde{n}^e_{\mathcal{K}} - \tilde{n}^s_{\mathcal{K}-\Delta,\uparrow}\tilde{n}^s_{\mathcal{K},\downarrow}\right] \right\} \qquad (3)$$

which describes spin ($\tilde{s}_{\mathcal{K}\sigma}$; $S^z_{\mathcal{K}} = \pm 1/2$, $C_{\mathcal{K}} = 0$) and charge ($\tilde{d}_{\mathcal{K}}, \tilde{e}_{\mathcal{K}}$; $S_{\mathcal{K}} = 0$, $C^z_{\mathcal{K}} = \pm 1/2$) degrees of freedom in an occupation number representation with a hard core constraint, $\sum_\sigma \tilde{n}^s_{\mathcal{K},\sigma} + \tilde{n}^d_{\mathcal{K}} + \tilde{n}^e_{\mathcal{K}} = 1$ for each $\mathcal{K}$. Furthermore, $h^s_{\mathcal{K},\sigma} = (t\mathcal{K})/2 - \mu_\sigma$, $h^d_{\mathcal{K}} = -(t\mathcal{K})/2 - 2\mu + U$, $h^e_{\mathcal{K}} = -(t\mathcal{K})/2$, and $J_{\mathcal{K}} = \left[t(2\mathcal{K}-\Delta) - U + \sqrt{(2\pi t)^2 + U^2 - 2tU(2\mathcal{K}-\Delta)}\right]/2 \geq 0$. The chemical potential in the presence of an external magnetic field is given by $\mu_\sigma = \mu -$

$\sigma(g\mu_B\mathcal{H}_0)/2$. In the following we will set $\mu_B \equiv 1$, and $g = 2$. To be precise, we also restrict ourselves to $t \geq 0$ and $U \geq -2\pi t$ in which case we were allowed to identify $\mathcal{K}_{\min} - \Delta \equiv \mathcal{K}_{\max}$ because $J_{\mathcal{K}}$ vanishes for $\mathcal{K} = \mathcal{K}_{\min} = -\Delta(L-1)/2$.

Note that, formally, the entire spectrum *appears* to display spin-charge separation *at all energies* in the sense that the Hamiltonian splits up into independent spin and charge contributions ("strong" spin-charge separation). In reality, however, spin and charge excitations are coupled by the constraint, $\sum_\sigma \widetilde{n}^s_{\mathcal{K},\sigma} + \widetilde{n}^d_{\mathcal{K}} + \widetilde{n}^e_{\mathcal{K}} = 1$; and spin-charge separation only occurs at sufficiently low energies/temperatures, where spin and charge excitations contribute independently to various physical properties.

As already discussed above, we will concentrate on the physics of two special limits: (i) the $1/r$-Hubbard model in the vicinity of half filling, $n \lesssim 1$, and (ii) the $1/r$-tJ model for $n < 1$. The latter is obtained by taking the limit $U \to \infty$ of (3) which projects out all double occupancies ($h^d_{\mathcal{K}} \to \infty$). With the help of the completeness constraint one arrives at the tJ effective Hamiltonian,

$$\hat{H}^{\text{eff}}_{\text{tJ}} = \hat{H}^{\text{eff}}_{\text{t}} + \hat{H}^{\text{eff}}_{\text{J}} = \sum_{-\pi<\mathcal{K}<\pi} \left[(-t\mathcal{K})\widetilde{n}^e_{\mathcal{K}} - J_{\mathcal{K}}\widetilde{n}^s_{\mathcal{K}-\Delta,\uparrow}\widetilde{n}^s_{\mathcal{K},\downarrow}\right], \tag{4}$$

where, for $J = 4t^2/U \ll 1$, the exchange coupling, $J_{\mathcal{K}}(U/t)$, reduces to $J_{\mathcal{K}} = (J/4)\left[\pi^2 - (\mathcal{K} - \Delta/2)^2\right]$. Below, we will adopt the usual standpoint for the tJ model[7], and treat J as an *independent* parameter.

A. 1/r-Hubbard Model

From eq. (3) we can immediately extract the form of eigenstates in an occupation number representation in terms of the effective spin ($\widetilde{s}_{\mathcal{K},\sigma}$) and charge ($\widetilde{e}_{\mathcal{K}}, \widetilde{d}_{\mathcal{K}}$) degrees of freedom. For example, the ground state is expressed symbolically as

$$\text{ground state:} \quad [\uparrow\downarrow]\ldots[\uparrow\downarrow]\Big|_{\mathcal{K}_F=\pi(2n-1)} \circ\ldots\circ$$

where $\uparrow$, $\downarrow$, $\bullet$, and $\circ$ represent $\widetilde{s}_{\mathcal{K},\uparrow}$, $\widetilde{s}_{\mathcal{K},\downarrow}$, $\widetilde{d}_{\mathcal{K}}$, $\widetilde{e}_{\mathcal{K}}$, respectively. We brace those pairs at $\mathcal{K} - \Delta$ and $\mathcal{K}$ which contribute an interaction $J_{\mathcal{K}}$ [8]. The ground state can be regarded as a short-range RVB state in $\mathcal{K}$-space obtained by filling $\mathcal{K}$ states with $[\uparrow\downarrow]$-pairs from $\mathcal{K} = -\pi + \Delta/2$ to $\mathcal{K} = \mathcal{K}_F - \Delta/2$, where $\mathcal{K}_F = \pi(2n-1)$. Although the real-space structure of the ground state wave function is not immediately apparent, it should be clear, however, that it also consists of long-range (overlapping) singlet pairs. In fact, the recently constructed wave functions for the $U = \infty$ limit (the "$1/r$-t-model")[9] are genuine RVB states[10] of the Gutzwiller-Jastrow type.

The corresponding ground state energy density, $e_0(n)$, can easily be obtained by applying the effective Hamiltonian (3) to the symbolic ground state wave function given above: $e_0(n) = (1/2\pi)\int_{-\pi}^{\mathcal{K}_F} d\mathcal{K}\,[J(\mathcal{K})/2] + (1/2\pi)\int_{\mathcal{K}_F}^{\pi} d\mathcal{K}(-t\mathcal{K})$, where the factor 1/2 in the first term takes into account the fact that only every second $\mathcal{K}$ value contributes to the first integral. A simple calculation then gives

$$e_0(n \le 1) = \frac{Un - W(1-n)n}{4} - \frac{1}{24WU}\left[(W+U)^3 - \left((W+U)^2 - 4WUn\right)^{3/2}\right], \qquad (5)$$

where $W = 2\pi t$ is the bandwidth. Using particle-hole symmetry[11] we obtain $e_0(n \ge 1) = e_0(2-n) + U(n-1)$, and correspondingly, for the chemical potential at zero temperature, $\mu(n<1) = \partial e_0(n<1)/\partial n$, $\mu(n>1) = U - \mu(2-n)$. From (5) one can easily see that $\Delta\mu_c \equiv \mu_+(n=1) - \mu_-(n=1) = (\lim_{n\to 1^+} - \lim_{n\to 1^-})\mu(n)$ becomes finite for $U > U_c = W$: $\Delta\mu_c = U - U_c$. Equivalently, the charge compressibility, $\kappa = \partial n/\partial\mu$ at $n=1$ vanishes for U above U_c, as expected at a Mott metal-to-charge-insulator transition (MCIT).

We are now in the position to identify the low-lying spin and charge excitations which we discuss separately for the half-filled and less than half-filled cases:

1. Half-filling: $n = 1$

We begin with the *spin excitations.* The four degenerate $S=0$, $S=1$ lowest-lying spin excitations are represented by

$$\text{spin-exc:}\quad [\uparrow\downarrow]\ldots[\uparrow\downarrow]\,\sigma\Big|_{\mathcal{K}_1}[\uparrow\downarrow]\ldots[\uparrow\downarrow]\,\sigma'\Big|_{\mathcal{K}_2}[\uparrow\downarrow]\ldots[\uparrow\downarrow]\quad .$$

For $\mathcal{K}_2 = \mathcal{K}_1 + \Delta$ there is a triplet excitation only. In the thermodynamic limit the excitation energy is given by $\delta E_S(\mathcal{K}_1, \mathcal{K}_2) = [J(\mathcal{K}_1) + J(\mathcal{K}_2)]/2$, and we may thus identify the lowest-lying spin excitation with two *spinons*. They are characterized as spin-1/2 objects which always come in pairs, and are separated in $\mathcal{K}$-space by an *even multiple* of Δ. We thus rescale $\mathcal{K} = 2\mathcal{K}'$ to retain the proper spacing $\Delta = 2\pi/L$ of $\mathcal{K}'$ values. The spinons then have the dispersion relation,

$$\epsilon_s(\mathcal{K}) = J(2\mathcal{K})/2 = \left(\sqrt{W^2 + U^2 - 4WU\mathcal{K}/\pi} + 2W\mathcal{K}/\pi - U\right)/4 \geq 0 \quad ; \quad |\mathcal{K}| < \pi/2\,, \tag{6}$$

which we depict in fig. 1. The spin excitations are always gapless at $\mathcal{K} = -\pi/2$, and at $\mathcal{K} = \pi/2$ for $U/W > 1$. Their corresponding velocities at $\mathcal{K} = \pm\pi/2$ can now be calculated from $v_s(\mathcal{K}) = \partial\epsilon_s(\mathcal{K})/\partial\mathcal{K}$ as

$$v_s^R \equiv v_s(\mathcal{K} = -\pi/2) = \frac{v_F}{U/W + 1} \quad \text{for all} \quad U/W \tag{7a}$$

$$v_s^L \equiv v_s(\mathcal{K} = \pi/2) = -\frac{v_F}{U/W - 1} \quad \text{for} \quad U/W > 1 \quad . \tag{7b}$$

Here, $v_F = t$ is the Fermi velocity of the bare particles. The density of states for *spin excitations* is then calculated as $D_s(E) = (1/L)\sum_{-\pi/2<\mathcal{K}<\pi/2} \delta\left(E - \epsilon_s(\mathcal{K})\right) = 1/(2\pi)\int_{-\pi/2}^{\pi/2} d\mathcal{K}\, \delta\left(E - \epsilon_s(\mathcal{K})\right)$. With the help of eqs. (7), for low energies we obtain

$$D_s(E \to 0) = \begin{cases} 1/\left(2\pi v_s^R\right) & \text{for } U/W < 1 \\ 1/\left(2\pi v_s^R\right) + 1/\left(2\pi |v_s^L|\right) & \text{for } U/W > 1 \end{cases} \quad . \tag{8}$$

We next turn to the *charge excitations*. We restrict ourselves to a fixed particle number ($C^z = 0$) and we only obtain two of the four $C = 0$, $C = 1$ lowest-lying states. These charge excitations are represented by

$$\text{charge-exc:} \quad [\uparrow\downarrow]\ldots[\uparrow\downarrow] \circ\Big|_{\mathcal{K}_1} [\uparrow\downarrow]\ldots[\uparrow\downarrow] \bullet\Big|_{\mathcal{K}_2} [\uparrow\downarrow]\ldots[\uparrow\downarrow] \quad .$$

For $\mathcal{K}_2 = \mathcal{K}_1 + \Delta$ there is a low lying triplet excitation ($C = 1$, $C^z = 0$), with the singlet excitation ($C = 0$, $C^z = 0$) always at high energy (anti-bound state). Again, we may identify the lowest-lying charge excitation with two *chargeons*. In the half-filled case we always get a pair of a *holon* and a *doublon* which are separated by an even multiple of $\Delta = 2\pi/L$. Rescaling $\mathcal{K} = 2\mathcal{K}'$ leads to the chargeon dispersion relation,

$$\epsilon_c(\mathcal{K}) = \left(\sqrt{W^2 + U^2 - 4WU\mathcal{K}/\pi} - 2W\mathcal{K}/\pi + U\right)/4 \geq 0 \quad ; \quad |\mathcal{K}| < \pi/2 \quad , \tag{9}$$

as depicted in fig. 1. The charge excitations are gapless at $\mathcal{K} = \pi/2$ for $U/W < 1$, with a velocity given by

$$v_c^L = -\frac{v_F}{1 - U/W} \quad \text{for} \quad U/W < 1 \quad . \tag{10}$$

For $U > W$ a gap, $2\epsilon_c(\pi/2) = U - W \equiv \Delta\mu_c$, opens in the charge spectrum. Correspondingly, the density of states for *charge excitations* at low energies takes the form

$$D_c(E \to 0) = \begin{cases} 1/\left(2\pi|v_c^L|\right) & \text{for } U/W < 1 \\ \mathcal{O}\left[\exp\left(-E/\Delta\mu_c\right)\right] & \text{for } U/W > 1 \end{cases} \quad . \tag{11}$$

At this point a peculiarity of our model becomes evident: the charge velocity *increases* as a function of U/W and eventually diverges at $U = U_c = W$. The effective charge mass m_c^* which is connected to the density of states or the velocities by $m_c^*/m = D_c(0)/D_0(0) = v_F/|v_c^L|$ *decreases* as a function of U/W. This is in contrast to the Brinkman-Rice scenario for the Mott-Hubbard transition in that case m_c^*/m *increases* and charge excitations tend to localize close to the transition[12,13]. Indeed, for the Hubbard model with nearest-neighbor hopping (cosine dispersion) $m_c^*(n, U)$ diverges at the MCIT for $U > 0$ when the transition is approached from below half-filling ($n \to 1^-$)[14].

2. Less than half-filling: $n < 1$

In this case there are only right-moving spinons with velocity v_s^R, eq. (7a). The spinons are further restricted to $-\pi/2 < \mathcal{K} < \mathcal{K}_F/2$ with $\mathcal{K}_F = \pi(2n - 1)$. The lowest-lying charge excitations are now given by *holons* alone while the doublons are always gaped:

$$\text{charge-exc:} \quad [\uparrow\downarrow]\ldots[\uparrow\downarrow]\circ\Big|_{\mathcal{K}}[\uparrow\downarrow]\ldots[\uparrow\Big|_{\mathcal{K}_F}\downarrow]\circ\ldots\circ \ .$$

Although holons need not come in pairs, they are still separated by an even multiple of Δ in $\mathcal{K}$-space. Rescaling again we find for the charge excitation

$$\epsilon_h(\mathcal{K}) = \epsilon_s(\mathcal{K}) - \epsilon_s(\mathcal{K}_F/2) + t(\mathcal{K}_F - 2\mathcal{K}) \quad -\pi/2 < \mathcal{K} < \mathcal{K}_F/2 \quad . \tag{12}$$

The holons are gapless at $\mathcal{K} = \mathcal{K}_F/2$, and the corresponding velocity, $v_c^L = \partial\epsilon_h(\mathcal{K})/\partial\mathcal{K}\Big|_{\mathcal{K}_F/2}$, leads to

$$v_c^L = -v_F\left(1 + \frac{U}{\sqrt{(W+U)^2 - 4WUn}}\right) \quad . \tag{13}$$

In turn, this implies that the density of states for charge excitations at low energies still remains

$$D_c(E \to 0) = \frac{1}{2\pi|v_c^L|} \quad . \tag{14}$$

3. Ground-state compressibility and magnetic susceptibility

The results for the ground state energy density $e_0(n)$, eq. (5), allow us to calculate the chemical potential $\mu = \partial e_0(n)/\partial n$ and the $T = 0$ compressibility $\kappa = \partial n/\partial\mu$. By turning on a small external magnetic field $\mathcal{H}_0$ we can also obtain $e_0(m,n)$ (see Appendix A, eq. (A4)), and the magnetic susceptibility, $\chi = \partial m/\partial\mathcal{H}_0$, where the magnetization density, m, is related to $\mathcal{H}_0$ by $\mathcal{H}_0 = \partial e_0(m,n)/\partial m$. We summarize our results as follows:

(i) $n < 1$ or ($n = 1$, $U/W < 1$):

$$\mu = \frac{U - W(1-2n) - \sqrt{(W+U)^2 - 4WUn}}{4} \tag{15a}$$

$$\kappa = \frac{1}{\pi|v_c^L|} = \frac{2}{W\left(1 + U/\sqrt{(W+U)^2 - 4WUn}\right)} \tag{15b}$$

$$m = \chi\mathcal{H}_0 \tag{15c}$$

$$\chi = \frac{1}{\pi v_s^R} = \frac{2}{W}\left(1 + \frac{U}{W}\right) \quad . \tag{15d}$$

(ii) $n = 1$, $U/W > 1$:

$$\mu(n = 1^-) = \frac{W}{2} \tag{16a}$$

$$\mu(n = 1^+) = U - \frac{W}{2} \tag{16b}$$

$$\Delta\mu_c = U - W \tag{16c}$$

$$\kappa = 0 \tag{16d}$$

$$m = \chi\mathcal{H}_0 \tag{16e}$$

$$\chi = \frac{1}{\pi v_s^R} + \frac{1}{\pi|v_s^L|} = \frac{4U}{W^2} \quad . \tag{16f}$$

The system is an incompressible charge insulator at half-filling and $U > W$. Note that in the limit $n \to 1^-$ the compressibility stays *finite* for $U > W$ (for $U = W$, $\kappa = 4\sqrt{1-n}/W$ for $n \lesssim 1$). This is, nevertheless, consistent with eq. (16d) since, in contrast with the situation of the usual Hubbard model[15,14], in our case the function $n(\mu)$ is not differentiable at $\mu(n = 1^-)$ and $\mu(n = 1^+)$.

We further note that eqs. (15b), (15d), and (16f) are the generic behavior expected of a "Luttinger-Liquid"[16], a point which we exploit in our discussion of the ground-state correlation functions (sec. IV) and the Drude conductivity (sec. V).

B. 1/r-tJ Model

Since the case of half-filling has already been considered by Haldane[17], here we will be mainly interested in the less that half-filled situation. From the effective tJ Hamiltonian (4) it is easy to see that the hole kinetic energy favors all particles to be as close to $\mathcal{K} = -\pi$ as possible while the exchange interaction $J_{\mathcal{K}} = (J/4)\left[\pi^2 - (\mathcal{K} - \Delta/2)^2\right]$ tries to distribute the particles symmetrically around $\mathcal{K} = 0$. We thus expect a transition at some critical J_c in this case.

In general, the ground state can be represented as

$$\text{ground state:} \quad \circ\ldots\circ\Big|_{\mathcal{K}_1}[\uparrow\downarrow]\ldots[\uparrow\downarrow]\Big|_{\mathcal{K}_2}\circ\ldots\circ$$

where $\mathcal{K}_2 = \mathcal{K}_1 + 2\pi n$ has to be determined from the minimization of the ground state energy. We find (see appendix A)

$$\begin{aligned} e_0(n, J \leq J_c) &= -\frac{Wn(1-n)}{2} - \frac{J\pi^2 n^2(3-2n)}{12} \\ &= -\frac{J_c \pi^2 n}{12}\left[\left(\frac{J}{J_c} - 1\right) n(3-2n) + 3 - 3n + n^2\right] \end{aligned} \tag{17a}$$

with $\mathcal{K}_1 = -\pi$ and

$$\begin{aligned} e_0(n, J \geq J_c) &= -\frac{W^2 n}{2\pi^2 J} - \frac{J\pi^2 n(3-n^2)}{24} \\ &= -\frac{J_c^2 \pi^2 n}{24J}\left[\left(3-n^2\right)\left(\frac{J^2}{J_c^2} - 1\right) + 2\left(3 - 3n + n^2\right)\right] \end{aligned} \tag{17b}$$

with $\mathcal{K}_1 = -\pi\left(n + 2W/(\pi^2 J)\right) > -\pi$. Here, $J_c = 2W/(\pi^2(1-n))$ is the critical coupling. Note that J_c is proportional to $1/(1-n)$, i.e., it decreases with increasing (hole) doping. Below we discuss the two cases, $J < J_c$ and $J > J_c$, separately:

1. $J < J_c$

For $J < J_c$ we can make use of the $1/r$-Hubbard model results (sec. II A). In particular, $\epsilon_s(\mathcal{K}) = J((\pi/2)^2 - \mathcal{K}^2)/2$ for $-\pi/2 < \mathcal{K} < \mathcal{K}_F/2$, and the spinon velocity at $\mathcal{K} = -\pi/2$ is

$$v_s^R = J\pi/2 \quad . \tag{18}$$

It is amusing to note that this is precisely the result for the Heisenberg-chain with *nearest-neighbor* interactions[18]. This is consistent with the fact that the Gutzwiller projected Fermi sea $|\psi_0\rangle = \hat{P}_{D=0}|\text{Fermi-sea}\rangle$[19], the ground state wave function of the $1/r$-tJ model, is also an excellent trial state for the Heisenberg chain with nearest neighbor interaction[20,21], as well as for the nearest neighbor supersymmetric tJ model ($J = 2t$)[22]. As in sec. II A the corresponding low energy density of states is given by

$$D_s(E \to 0) = \frac{1}{2\pi v_s^R} \quad \text{for} \quad J < J_c \quad . \tag{19}$$

For $0 < J < J_c$, the holon velocity is calculated as

$$v_c^L = -\left(2t + J\pi(2n-1)/2\right) = -(\pi/2)\left[(1-n)\left(J_c - J\right) + nJ\right]. \tag{20}$$

Note that the limit $J \to 0$ is peculiar: precisely *at* $J = 0$ we have a free gas of holons with $\epsilon_h(\mathcal{K}, J = 0) = -2t(\mathcal{K} - \mathcal{K}_F/2)$ for $-\pi/2 < \mathcal{K} < \mathcal{K}_F/2$, but with allowed $\mathcal{K}$-values spaced by $\Delta/2$. On the other hand, the limit $J \to 0$ only gives *half* of the excitations since the $\mathcal{K}$ values are now spaced by Δ rather than $\Delta/2$. This is because, for $J > 0$, half of the $J = 0$ excitations develop a gap, corresponding to the energy required to break a spinon pair, $J(\mathcal{K}_F) > 0$. Consequently, the low energy density of states for charge excitations,

$$D_c(E \to 0) = \frac{1}{2\pi|v_c^L|} \quad \text{for} \quad 0 < J < J_c \quad , \tag{21}$$

is only half as big for $J \to 0$ as for $J = 0$.

2. $J > J_c$

For $J > J_c$ the lowest-lying spin excitation can be represented as

$$\text{spin-exc:} \quad \circ \ldots \circ\, \sigma \Big|_{\mathcal{K}} \circ \ldots \circ\, \sigma' \Big|_{\mathcal{K}'} \circ \ldots \circ \Big|_{\mathcal{K}_1} [\uparrow\downarrow] \ldots [\uparrow\downarrow] \circ \circ \Big|_{\mathcal{K}_2} \circ \ldots \circ \quad .$$

In the present case nothing can be said about the ground state wave function in terms of the original Fermions, since the link to the $1/r$-Hubbard model can no longer be made. Again, the spinons come in pairs but they can now have *arbitrary* separation in the region outside of $\mathcal{K}_1 < \mathcal{K}, \mathcal{K}' < \mathcal{K}_2$. A single spinon has the excitation energy $\epsilon_s(\mathcal{K}) = t(\mathcal{K} - \mathcal{K}_2) + J(\mathcal{K}_2)/2 = t(\mathcal{K} - \mathcal{K}_1) + J(\mathcal{K}_1)/2$ and thus, a *gap* proportional to $J - J_c$ opens in spinon spectrum:

$$\begin{aligned} \Delta\mu_s &= 2\epsilon_s(-\pi) \\ &= \frac{\pi^2(1-n)}{4}\left(1 - \frac{J_c}{J}\right)\left[J(1+n) - J_c(1-n)\right]. \end{aligned} \tag{22}$$

$J = J_c$ then corresponds to the onset of a metal-to-spin-insulator transition (MSIT).

For $J > J_c$ a charge excitation is represented by

$$\text{charge-exc.:} \quad \circ \ldots \circ\, [\uparrow \Big|_{\mathcal{K}_1} \downarrow] \ldots [\uparrow\downarrow] \circ \Big|_{\mathcal{K}} [\uparrow\downarrow] \ldots [\uparrow\downarrow] \Big|_{\mathcal{K}_2} \circ \ldots \circ$$

and, after rescaling $\mathcal{K}$, the excitation energy for $\mathcal{K}_1/2 < \mathcal{K} < \mathcal{K}_2/2$ is $\epsilon_h(\mathcal{K}) = t(\mathcal{K}_2 - 2\mathcal{K}) + (J(2\mathcal{K}) - J(\mathcal{K}_2))/2$. The corresponding velocities are

$$v_c^R = -v_c^L = J\pi n/2 \tag{23}$$

at $\mathcal{K} = \mathcal{K}_1/2$ and $\mathcal{K} = \mathcal{K}_2/2$, respectively. We see that, for low energies, the gapless excitations are *parity-symmetric* although the underlying Hamiltonian itself does *not* conserve parity. The low energy density of states for charge excitations,

$$D_c(E \to 0) = \frac{1}{2\pi v_c^R} + \frac{1}{2\pi |v_c^L|} = \frac{2}{J\pi^2 n} \quad \text{for} \quad J > J_c \quad . \tag{24}$$

doubles at the MSIT.

3. Ground-state compressibility and magnetic susceptibility

The $T = 0$ chemical potential, compressibility, magnetization, and magnetic susceptibility can be calculated from eqs. (17), (A5), (A8), and (A9) of appendix A . As in the case of the $1/r$-Hubbard model we summarize our results ($J_c = 2W/(\pi^2(1-n))$):

(i) $J < J_c$:

$$\begin{aligned} \mu &= -\frac{W(1-2n)}{2} - \frac{J\pi^2 n(1-n)}{2} \\ &= -\frac{\pi^2(1-n)J_c}{4}\left[2n\left(\frac{J}{J_c} - 1\right) + 1\right] \end{aligned} \tag{25a}$$

$$\kappa = \frac{1}{\pi |v_c^L|} = \frac{2}{\pi^2\left[(1-n)(J_c - J) + nJ\right]} \tag{25b}$$

$$m = \chi \mathcal{H}_0 \tag{25c}$$

$$\chi = \frac{1}{\pi v_s^R} = \frac{2}{\pi^2 J} \quad . \tag{25d}$$

(ii) $J > J_c$:

$$\begin{aligned} \mu &= -\frac{W^2}{2\pi^2 J} - \frac{J\pi^2}{8}(1-n^2) \\ &= -\frac{\pi^2 J_c^2(1-n)}{8J}\left[(1+n)\left(\frac{J^2}{J_c^2} - 1\right) + 2\right] \end{aligned} \tag{26a}$$

$$\kappa = \frac{1}{\pi v_c^R} + \frac{1}{\pi |v_c^L|} = \frac{4}{J\pi^2 n} \tag{26b}$$

$$\Delta\mu_s = \frac{\pi^2(1-n)}{4}\left(1 - \frac{J_c}{J}\right)[J(1+n) - J_c(1-n)] \tag{26c}$$

$$m = 0 \quad \text{for} \quad \mathcal{H}_0 < \mathcal{H}_0^c = \Delta\mu_s/2 \tag{26d}$$

$$\chi = 0 \quad . \tag{26e}$$

The system is a spin insulator for $J/J_c > 1$. Note that the compressibility κ doubles at the transition because another low-energy charge excitation replaces the spin mode which becomes gaped at $J = J_c$.

III. THERMODYNAMICAL PROPERTIES

As noted in Ref. 1, the effective Hamiltonian, (3), is equivalent to a *classical* Ashkin-Teller type model in the presence of an inhomogeneous "magnetic field"[23], with periodic boundary conditions. The thermodynamic properties of our system can then be calculated by transfer-matrix techniques[24]. We define the abbreviations $S_{\mathcal{K},\sigma} = \exp\left(-\beta h^s_{\mathcal{K},\sigma}\right)$, $D_{\mathcal{K}} = \exp\left(-\beta h^d_{\mathcal{K}}\right)$, $E_{\mathcal{K}} = \exp\left(-\beta h^e_{\mathcal{K}}\right)$, and $P_{\mathcal{K}} = \exp\left(-\beta J_{\mathcal{K}}\right)$ where $\beta = 1/k_BT$ ($k_B \equiv 1$) is the inverse temperature. The transfer matrix between sites $\mathcal{K} - \Delta$ and $\mathcal{K}$,

$$F_{\mathcal{K}-\Delta,\mathcal{K}} = \begin{pmatrix} S_{\mathcal{K},\uparrow} & S_{\mathcal{K},\downarrow}P_{\mathcal{K}}^{-1} & D_{\mathcal{K}} & E_{\mathcal{K}} \\ S_{\mathcal{K},\uparrow} & S_{\mathcal{K},\downarrow} & D_{\mathcal{K}} & E_{\mathcal{K}} \\ S_{\mathcal{K},\uparrow} & S_{\mathcal{K},\downarrow} & D_{\mathcal{K}} & E_{\mathcal{K}}P_{\mathcal{K}} \\ S_{\mathcal{K},\uparrow} & S_{\mathcal{K},\downarrow} & D_{\mathcal{K}} & E_{\mathcal{K}} \end{pmatrix} \quad ,$$

has two vanishing eigenvalues; the remaining two eigenvalues are given by

$$\lambda_{\mathcal{K}}^{\pm} = \frac{1}{2}\left[X_{\mathcal{K}} \pm \sqrt{X_{\mathcal{K}}^2 - 4\left[S_{\mathcal{K},\uparrow}S_{\mathcal{K},\downarrow}\left(1 - P_{\mathcal{K}}^{-1}\right) + D_{\mathcal{K}}E_{\mathcal{K}}\left(1 - P_{\mathcal{K}}\right)\right]}\right] \quad ,$$

where we introduced the abbreviation $X_{\mathcal{K}} = S_{\mathcal{K},\uparrow} + S_{\mathcal{K},\downarrow} + D_{\mathcal{K}} + E_{\mathcal{K}}$. The partition function for all chemical potentials μ, magnetic fields $\mathcal{H}_0$, interaction strengths U/W, and temperatures T,

$$\mathcal{Z}_L = \left(\prod_{-\pi<\mathcal{K}<\pi} {\lambda_{\mathcal{K}}}^{+} \right) + \left(\prod_{-\pi<\mathcal{K}<\pi} {\lambda_{\mathcal{K}}}^{-} \right) \quad , \tag{27}$$

leads, in the thermodynamic limit ($N_\sigma, L \to \infty$, $n_\sigma = N_\sigma/L =$ fixed), to the free energy density $f(\mu, \mathcal{H}_0, U/W, T) = \lim_{L\to\infty} [-\ln \mathcal{Z}_L/(\beta L)]$,

$$f(\mu, \mathcal{H}_0, U/W, T) = -\frac{1}{\beta} \int_{-\pi}^{\pi} \frac{d\mathcal{K}}{2\pi} \ln {\lambda_{\mathcal{K}}}^{+} \quad . \tag{28}$$

Here we made use of the fact that ${\lambda_{\mathcal{K}}}^{-} < {\lambda_{\mathcal{K}}}^{+}$ [25]. This general form (28) remains valid for the $1/r$-tJ model (2) if we set $D_{\mathcal{K}} \equiv 0$. From eq. (4) it is easy to see that at half-filling the problem is equivalent to an Ising model on a ring with nearest-neighbor coupling, $J_{\mathcal{K}} = (J/4)(\pi^2 - (\mathcal{K} - \Delta/2)^2)$, and one thus recovers all of Haldane's results for the spin-chain[17].

A. 1/r-Hubbard model at half filling

First note that at half-filling ($n = 1$, i.e.[11], $\mu(T) = U/2$) without external field the spectrum is completely specified in terms of *independent* spin and charge excitations. In fact, the free-energy in that case has the simple spin-charge separated form

$$\begin{aligned} f(n = 1, U/W, T) &= -U/2 + e_0(n = 1) \\ &\quad - \frac{2}{2\pi\beta} \int_{-\pi/2}^{\pi/2} d\mathcal{K} \left\{ \ln\left[1 + \exp\left(-\beta\epsilon_s(\mathcal{K})\right)\right] + \ln\left[1 + \exp\left(-\beta\epsilon_c(\mathcal{K})\right)\right] \right\} \end{aligned} \tag{29}$$

where the dispersion relations for the spin ("up" and "down" spinons) and charge (holons and doublons) excitations were already given in eqs. (6), (9) (see figure 1). Note that the rescaling of $\mathcal{K}$-values gives an additional factor of two in front of the integral such that (29) corresponds to the result of two independent free fermion systems for charge and spin.

1. Specific heat

The spinon and chargeon densities of states, $D_{s,c}(E) = 1/(2\pi) \int_{-\pi/2}^{\pi/2} d\mathcal{K} \delta\left(E - \epsilon_{s,c}(\mathcal{K})\right)$, are shown in figure 2a and 2b, respectively. Already before the MCIT the density of states for the spinons develops a van-Hove singularity at $U = W/2$. This could be interpretated as the formation of the lower (spinon) and upper (chargeon) Hubbard band which are, however, not yet separated.

Given the densities of states, the internal energy density $u(n=1,T)$ can be obtained from $u(n=1,T) = e_0(n=1) + 2\int_0^\infty dE\,[D_s(E) + D_c(E)]\,Ef(E)$, where $f(E) = [\exp(\beta E) + 1]^{-1}$ is the Fermi-Dirac distribution function. The specific heat $c_v = -\beta^2 \partial u/\partial\beta$ is then given by

$$c_v(n=1,T) = 4T \int_0^\infty dx\,(D_s(2xT) + D_c(2xT)) \left(\frac{x}{\cosh x}\right)^2 \quad . \tag{30}$$

At low temperatures this reduces to $c_v(n=1, T\to 0) = \gamma(n=1)T$ with

$$\gamma(n=1) = \frac{\pi^2}{3}\,[D_s(0) + D_c(0)] \quad . \tag{31}$$

This Luttinger Liquid relation[16], which remains valid for all fillings, will allow us to identify the conformal charge of the conformal field theory that governs the low energy behavior of our model (see sec. IV).

The behavior of the Sommerfeld coefficient γ as a function of the interaction parameter, U/W, can be extracted from eqs. (7), (8), (10), and (11):

$$\gamma(n=1) = \frac{\pi^2}{3} D_0(0) \begin{cases} 1 & \text{for } U/W < 1 \\ U/W & \text{for } U/W > 1 \end{cases} \tag{32}$$

where $D_0(0) = 2/W$ is the non-interacting density of states. Note that $\gamma(n=1)$ is *unrenormalized* below the MCIT. The reason is that the *increase* in the density of states for spin excitations is exactly compensated by the *decrease* in the density of states for the charge excitations. This precise cancellation of the two contributions is a peculiarity of our model and does not occur in the conventional Hubbard model. In a realistic scenario for the Mott-Hubbard transition we expect a growing effective charge mass (or, equivalently, $D_c(0)$) because the transport of charge becomes more difficult due to the Coulomb repulsion[14]. Also, the spin transport should become less effective because the spin exchange energy smoothly reduces from $\mathcal{O}(t)$ to $\mathcal{O}(J = 4t^2/U)$ and we thus also expect an increasing effective spin mass (or $D_s(0)$). Consequently, there should be an increase of γ below the MCIT in any realistic Hubbard-type model.

The specific heat as a function of temperature is shown in fig. 3. The general structure of $c_v(T)$ reflects the behavior of the density of states (see fig. 2). Even before the MCIT, at $U = W/2$, the specific heat develops a two peak structure which reflects the van-Hove singularity in the density of states for spin excitations. As already seen in eq. (32), the Sommerfeld factor is continuous at the transition. Well above the transition ($U >> W$) the lower and upper Hubbard bands are well separated, which is reflected in a narrow low-temperature peak in $c_v(T)$ and a broad maximum around $T = \mathcal{O}(U)$. In spite of the peculiarities of our model the overall shape of $c_v(T)$ is expected to be generic for any Hubbard model with a smooth dispersion relation, in the absence of perfect nesting.

2. Compressibility

Next we discuss the isothermal compressibility $\kappa(T) = \partial n/\partial\mu$ which is related to the particle number fluctuation by $\kappa(n = 1, T) = T\langle(\Delta\hat{N})^2\rangle/L = -\left(\partial^2/\partial\mu^2\right) f(\mu, T)\Big|_{\mu=U/2}$. Here, $\Delta\hat{N} \equiv \hat{N} - \langle\hat{N}\rangle$. A direct calculation gives

$$\kappa(n = 1, T) = \frac{\beta}{\pi}\int_{-\pi/2}^{\pi/2} d\mathcal{K}\left[\exp\left(-\beta\epsilon_s(\mathcal{K})\right) + \exp\left(\beta\epsilon_c(\mathcal{K})\right)\right]^{-1} \quad . \tag{33}$$

Note that the compressibility probes the system slightly away from half-filling. It is thus seen that not only the chargeon dispersion $\epsilon_c(\mathcal{K})$ but also the spinon dispersion $\epsilon_s(\mathcal{K})$ enters the expression for the compressibility. Therefore, strong charge-spin separation, in the sense of a completely decoupled response of charge and spin excitations to an external force, does not exist even at half-filling. It is only for $T \to 0$ that the spinons do not contribute to the compressibility (or holons to the magnetic susceptibility), as can be seen from eqs. (15b), (15d), and (16f).

The fluctuation of the particle density at half-filling is shown in figure 4. At low temperatures and below the MCIT the fluctuations are linear in temperature, i.e., the compressibility is constant and given by (15b). Above the transition the charge gap opens, and there are only exponentially small particle number fluctuations at low temperatures. At high temperatures the fluctuations saturate at $T\kappa(n=1, T\to\infty) = 1/2$. This is the classical value for spin-1/2 electrons on a lattice where on average half of the sites are doubly occupied or empty.

3. Magnetic susceptibility

The magnetic susceptibility at zero external magnetic field is given by $\chi(T) = -\left(\partial^2/\partial\mathcal{H}_0^2\right) f(\mathcal{H}_0, T)\Big|_{\mathcal{H}_0=0}$. It can be directly evaluated at half-filling in terms of both spinon and chargeon degrees of freedom as

$$\chi(n=1,T) = \frac{\beta}{\pi}\int_{-\pi/2}^{\pi/2} d\mathcal{K}\left[\exp\left(\beta\epsilon_s(\kappa)\right) + \exp\left(-\beta\epsilon_c(\mathcal{K})\right)\right]^{-1} \quad . \tag{34}$$

The result is plotted in figure 5. At low temperatures it shows Pauli behavior which is strongly enhanced by the interaction, especially above the MCIT (see eqs. (15d), (16f)). With increasing U/W, due to the enhanced density of spin excitations at low energies, the susceptibility develops a strong peak at low temperatures. At high temperatures the susceptibility shows Curie behavior, $\chi(n=1, T\to\infty) = 1/(2T)$, the classical value for spin-1/2 electrons on a lattice where on average half of the sites are singly occupied. This behavior of $\chi(T)$ is familiar from the Hubbard model with cosine dispersion at half-filling[15], and is thus a generic feature of Hubbard-type models.

B. 1/r-tJ model

Away from half-filling there is no compact representation of the free energy in terms of the spinon and chargeon dispersion and one must use the general form in eq. (28), with $D_{\mathcal{K}} \equiv 0$, and $P_{\mathcal{K}} = \exp\left(-\beta J\left(\pi^2 - \mathcal{K}^2\right)/4\right)$. Furthermore, the chemical potential now depends on both temperature and density. We will concentrate on a typical filling factor, $n = 0.75$, which corresponds to a critical value of the coupling $J_c/W = 0.81$.

1. Chemical potential

The chemical potential as a function of T for fixed $n = 0.75$ and various values of J/J_c is shown in figure 6. It is seen that $\mu(J,T)$ depends smoothly on T for $T/J_c < 1$. Both above and below the MSIT μ is only weakly temperature dependent at low temperatures, a behavior which is especially pronounced for larger values of J/J_c where it remains at its $T = 0$ value, eq. (26a), for all $T/J_c \leq 0.5$. Although $\mu(J,T)$ develops stronger T-dependence at low temperatures in the vicinity of the MSIT, it remains continuous as a function of J and shows no anomalies at $J = J_c$.

2. Specific heat

The specific heat as a function of T for fixed $n = 0.75$ and various values of J/J_c is shown in figure 7. There is just one maximum which gradually becomes broader and shifts to higher temperatures with increasing coupling strength J. More revealing features appear in the temperature dependence of the Sommerfeld coefficient $\gamma(T) = c_v(T)/T$, shown in fig. 8, which is nothing but $(\partial s/\partial T)$, the temperature derivative of the entropy. First of all, it is seen that the Luttinger Liquid relation $\gamma(T=0) = (\pi^2/3)(D_s(0) + D_c(0))$ remains valid (compare eqs. (19), (21), (24), and (31)). For low temperatures and just above the MSIT, $\gamma(T)$ shows a prominent peak, reflecting the large density of states for spin excitations just above the spin gap. As J becomes larger, this features broadens and shifts to higher temperatures and is completely washed out for $J/J_c \approx 2$.

3. Compressibility

Fig. 9 shows the isothermal compressibility $\kappa(n = 0.75, T)$ for several values of J/J_c, (a) below and (b) above the MSIT. For $J < J_c$ the compressibility decreases with increasing J, especially through the suppression of the peak at $T \approx 0.3J_c$. At the transition, the compressibility at $T = 0$ doubles because of the appearance of an extra gapless holon excitation in the spectrum (see sec. II B 3). Just below the transition this additional density of states for charge excitations is already present at low but finite energies and causes a sharp increase in the slope of $\kappa(T)$ for low temperatures such that the compressibility for $J/J_c = 0.99$ is actually higher than for $J/J_c = 0.74$ in a temperatures region around $T/J_c = 0.1$. Above the transition the additional density of states for gapless charge excitations results in a new low temperature peak, which broadens and shifts to higher temperatures (and is eventually completely suppressed) as J is further increased above the MSIT.

4. Magnetic susceptibility

Finally, fig. 10 shows the magnetic susceptibility $\chi(n = 0.75, T)$ for the $1/r$-tJ model for various values of J/J_c below and above the MSIT. The susceptibility can be cast into the form

$$\chi(\mu, T) = \frac{\beta}{\pi} \int_{-\pi}^{\pi} d\mathcal{K} \left\{ \exp\left[2\beta\left(t\mathcal{K} - \mu\right)\right] + 4\exp\left[\beta\left(t\mathcal{K} - \mu\right)\right] + 4\exp\left[\beta J\left(\pi^2 - \mathcal{K}^2\right)/4\right] \right\}^{-1/2} . \tag{35}$$

As expected, for $J < J_c$ we find a finite (Pauli) susceptibility at $T = 0$, eq. (25d). Evaluating the linear term in T from eq. (35) one finds $\chi(n, T \to 0) = 2/(J\pi^2) + [8/(J\pi^2)^2]\, T + \mathcal{O}(T^2)$, independent of $n < 1$. Close to the transition, however, the temperature region over which this expansion is valid shrinks to zero, and the susceptibility thus seems to have a negative temperature gradient at low temperatures close to the MSIT ($J/J_c = 0.99$). Just below the transition we have a strong increase in the density of states for charge excitations at low energies which already showed up in the compressibility. Consequently, the density of states for low-energy spin excitations is considerably reduced. This results in a low-temperature dip of the magnetic susceptibility close to the MSIT.

For $J > J_c$ the magnetic susceptibility shows activated behavior reflecting the opening of the spin gap, $\Delta\mu_s$ (eq. (22)). It is seen that the curves for $J/J_c = 0.99$ and $J/J_c = 1.02$ qualitatively differ from each other only in a region of very low temperatures ($T \lesssim 0.07 J_c$).

IV. CONFORMAL FIELD THEORY APPROACH AND CORRELATION FUNCTIONS

Since we do not know how to express the original electron operators in terms of the eigenstates of our effective Hamiltonian, we cannot directly calculate any correlation functions for our model. Fortunately, away from any phase transitions, our model belongs to the class of Luttinger Liquids[16] for which the low temperature/energy behavior is dominated by two gapless excitations for charge and spin with linear spectrum and *different* velocities v_s, v_c (charge-spin separation). It is then natural to attempt to calculate the low energy behavior of various correlation functions of our model by recasting our results within the framework of conformal field theory[26–29] and g-ology[14,30–32] techniques, both of which have proved extremely powerful in extracting the physics of the Luttinger Liquid fixed point. In this section we focus on the former approach and leave for the next section the discussion of g-ology.

It is well known that $T = 0$ can often be viewed as the "critical point" in two-dimensional classical or one-dimensional quantum field theories: correlation functions decay algebraically instead of exponentially for long times and/or distances, i.e., there is no intrinsic length scale. The *assumption* that, in addition to linearizing the fermionic spectrum, conformal invariance also holds at low energies/temperatures restricts the behavior of the lowest order $1/L$-corrections to the ground state energy density (E_0^L), and the energies ($E_{h^\pm}^L$) and momenta ($P_{h^\pm}^L$) of low-lying states of system of finite size, L. In turn, this information is sufficient to determine the long range, long time behavior of correlation functions. [An equivalent approach which is based on a Landau expansion around the ground state for Bethe-Ansatz solvable problems gives the same results[33]]. In particular, for a one component Fermi gas with a linear spectrum conformal invariance implies:

$$E_0^L - L\epsilon_0 = -\frac{\pi c v}{6L} \tag{36a}$$

$$E_{h^\pm}^L - E_0^L = \frac{2\pi}{L} v \left(N^+ + N^- + h^+ + h^- \right) \tag{36b}$$

$$P^L_{h^\pm} - P^L_0 = \frac{2\pi}{L}\left(h^+ - h^- + N^+ - N^-\right) + P^\infty_h \quad . \tag{36c}$$

Here, c is the conformal charge, v is the velocity of the the right- and left-moving elementary excitations, $h^\pm$ are their conformal dimensions, P^∞_h is the momentum of the sound excitations in the thermodynamic limit, and $N^\pm$ are integers[27–29].

A particularly simple way of determining the conformal charge from the Sommerfeld coefficient of the specific heat is due to Affleck[34]. For a one-component system with right- and left-moving elementary excitations

$$\gamma = \frac{\pi}{3}\frac{c}{v} = \frac{\pi^2}{3}cD(0), \tag{37}$$

where $D(0)$ is the density of states for low energies.

The information of eqs. (36) and (37) determines the large distance x, long-time t behavior of correlation functions of the (primary) fields $\Phi_{h^\pm}(x,t)$ as follows[27–29]

$$\langle \Phi_{h^\pm}(x,t)\Phi_{h^\pm}(0,0)\rangle = \frac{\exp\left(-iP^\infty_h x\right)}{(x-ivt)^{2h^+}(x+ivt)^{2h^-}} \quad . \tag{38}$$

We are interested in the long-range behavior of the spin-spin correlation function $C^{\mathrm{SS}}(r,t)$, the density-density correlation function $C^{\mathrm{NN}}(r,t)$, and the one-particle Green's function $G_\sigma(x,t)$,

$$C^{\mathrm{SS}}(r,t) = \frac{1}{L}\sum_{l=1}^{L}\langle(\hat{n}_{l+r,\uparrow}(t) - \hat{n}_{l+r,\downarrow}(t))\,(\hat{n}_{l,\uparrow} - \hat{n}_{l,\downarrow})\rangle \tag{39a}$$

$$C^{\mathrm{NN}}(r,t) = \left[\frac{1}{L}\sum_{l=1}^{L}\langle(\hat{n}_{l+r,\uparrow}(t) + \hat{n}_{l+r,\downarrow}(t))\,(\hat{n}_{l,\uparrow} + \hat{n}_{l,\downarrow})\rangle\right] - \left(\frac{n}{2}\right)^2 \tag{39b}$$

$$G_\sigma(r,t) = \frac{-i}{2\pi}\frac{1}{L}\sum_{l=1}^{L}\langle\mathcal{T}\hat{c}_{l,\sigma}\hat{c}^+_{l+r,\sigma}(t)\rangle \tag{39c}$$

where $\mathcal{T}$ is the time-ordering operator. The only remaining task in computing the asymptotic behavior of these correlation functions is identifying the appropriate (primary) fields associated with the physical operators of interest.

In what follows we use our exact results to carry out the procedure outlined above.

A. 1/r-Hubbard model

1. Conformal Charge

The obvious generalization of (37) to a two-component system with charge and spin excitations is to replace $D(0)$ by $(D_s(0) + D_c(0))$. As could have been expected, comparing with eq. (31) gives $c = 1$[35].

We note that, since this identification requires finite spin and charge velocities, it breaks down at the MIT. This could have been inferred from the excitation spectra for charge and spin (eqs. (6), (9)) which are no longer linear near $\mathcal{K} = \pi/2$ but behave as $\omega \propto k^\alpha$ with $\alpha = 1/2$. This is reflected in the finite size corrections to the ground state energy which behave as $\sqrt{1/L}$ instead of $1/L$. More precisely, from eq. (B3), one obtains for half-filling

$$(E_0^L - L\epsilon_0)(n=1) = \sqrt{\frac{1}{L}}\frac{W}{2}\sum_{s=1}^{\infty}(-1)^s\left(\frac{1}{\pi s}\right)^{3/2}\int_0^{\pi s L} dy \frac{\sin y}{\sqrt{y}} \quad . \tag{40}$$

A similar breakdown of conformal invariance occurs in the context of superintegrable chiral N-state Potts models[36] for $N \geq 3$.

It is also worth pointing out that, as shown in appendix B, even away from the transition, there are some *additive* corrections to the usual formula (36a) in our case. More precisely, we find

$$E_0^L - L\epsilon_0 = -\frac{\pi}{6L}\left[v_s^R - v_F + |v_c^L| - v_F\right] \tag{41}$$

(for $n = 1$ and $U > W$ one has to read v_s^L instead of v_c^L). It is easy to see that the corrections guarantee that there are *no* $1/L$ corrections present at $U = 0$ where $E_0 = L\epsilon_0$ is the exact result for all L. This requirement follows from the fact that in our case the entire spectrum of the kinetic energy operator $\hat{T}$ can be obtained from $N-1$ independent spin-1/2 SU(2) algebras in each sector with fixed total momentum Q: $\hat{T}_Q^N \equiv t(Q-\pi) + W\sum_{i=1}^{N-1}\hat{F}_i^z$ (N even). Thus, in this case the algebraic structure is much simpler than the usual Virasoro algebra[26,27]; this invalidates the conventional arguments based on conformal invariance and justifies the absence of finite size correction in the strict $U = 0$ limit.

2. Conformal dimensions

According to eqs. (36b), (36c), in order to identify the conformal dimensions we need to consider those lowest-lying states with the quantum numbers of the physical excitation of interest. We will consider two- and one-particle excitations which determine the long-range behavior of the spin-spin and density-density correlation functions, and one-particle Green's function, respectively.

a. $n < 1$*:* Away from the transition the lowest-lying two-spinon excitation is obtained from the ground state by breaking a $[\uparrow\downarrow]$-pair at $\mathcal{K} = -\pi + \Delta/2$ and $\mathcal{K} = -\pi + 3\Delta/2$, and placing the electrons into the $S = 1$, $S^z = 0$ state at the same $\mathcal{K}$ points. The corresponding excitation energy is

$$E^L_{h_s^+} - E^L_0 = J(\mathcal{K} = -\pi + 3\Delta/2) = \frac{2\pi}{L} v_s^R + \mathcal{O}\left(1/L^2\right) \quad , \tag{42}$$

corresponding to $h_s^+ = 1$ (only right-moving spinons). Furthermore,

$$P^L_{h_s^+} - P^L_0 = \pi + \frac{1}{2}\left[(-\pi + \Delta/2)\,(-\pi + 3\Delta/2)\right] = \frac{2\pi}{L} h_s^+ \tag{43}$$

where we took into account[1] that each bound spin-pair contributes a momentum of π, and each unbound spin at $\mathcal{K}$ adds $\mathcal{K}/2$. As a result, $P^\infty_{h_s^+} = 0$.

The charge excitation can be treated analogously and one finds (again for $n < 1$)

$$\begin{aligned} E^L_{h_c^-} - E^L_0 &= (-t)(\mathcal{K}_F - 3\Delta/2) + t(\mathcal{K}_F + \Delta/2) + J(\mathcal{K}_F - \Delta/2) - J(\mathcal{K}_F + \Delta/2) \\ &= \frac{2\pi}{L}|v_c^L| + \mathcal{O}\left(1/L^2\right) \end{aligned} \tag{44}$$

$$P^L_{h_c^-} - P^L_0 = \frac{1}{2}\left[-\left(\mathcal{K}_F - 3\Delta/2\right) + \left(\mathcal{K}_F + \Delta/2\right)\right] = \frac{2\pi}{L}, \tag{45}$$

implying $h_c^- = 1$, $P^\infty_{h_c^-} = 0$.

Finally, the one-particle excitation from the N-particle ground state is given by the $N + 1$-particle ground state:

$$\text{ground state } (N+1 \text{ particles}): \quad \sigma\,[\uparrow\downarrow]\ldots[\uparrow\Big|_{\mathcal{K}_F}\ \downarrow]\circ\ldots\circ$$

We then find,

$$E^L_{N+1,0} - E^L_{N,0} = t(\mathcal{K}_F + \Delta/2) + \sideset{}{'}\sum_{\mathcal{K}=-\pi+3\Delta/2}^{\mathcal{K}-\Delta/2} \Big(J(\mathcal{K}) - J(\mathcal{K}+\Delta) \Big)$$

$$= \mu(n) + \frac{2\pi}{L}\left[\frac{v_s^R}{4} + \frac{|v_c^L|}{4}\right] + \mathcal{O}\left(1/L^2\right) \tag{46}$$

$$P^L_{N+1,0} - P^L_{N,0} = \frac{1}{2}\left[(-\pi + \Delta/2) + (\mathcal{K}_F + \Delta/2)\right] = \frac{\pi}{L} + \pi(n-1) \quad , \tag{47}$$

and correspondingly, $h_N^c = h_N^s = 1/4$, $P_N^\infty = \pi(n-1) = k_F^e$ (k_F^e is the electronic Fermi momentum).

b. $n = 1$: Below the transition ($U/W < 1$) the same results as for $n < 1$ apply. Above the transition ($U/W > 1$) we have no gapless charge excitations. This implies that all correlation function involving charge excitations (density-density correlation function, one-particle Green's function) decay exponentially because their excitation energies always involve the charge gap $\Delta\mu_c$.

On the other hand, we have additional spin excitations. Besides the excitation with two right-moving spinons ($h_s^+ = 1$, $P^\infty_{h_s^+} = 0$) we also find the corresponding excitation with two left-moving spinons ($h_s^- = 1$, $P^\infty_{h_s^-} = 0$). Furthermore, we may split the two spinons to form the excited state

$$\text{spin-exc.:} \quad \sigma[\uparrow\downarrow]\dots[\uparrow\downarrow]\sigma'$$

leading to

$$E^L_{h_s^\pm} - E^L_0 = \sideset{}{'}\sum_{\mathcal{K}=-\pi+3\Delta/2}^{\pi-\Delta/2} J(\mathcal{K}) - \sideset{}{'}\sum_{\mathcal{K}=-\pi+5\Delta/2}^{\pi-3\Delta/2} J(\mathcal{K})$$

$$= \frac{2\pi}{L}\left[\frac{v_s^R}{4} + \frac{|v_c^L|}{4}\right] + \mathcal{O}\left(1/L^2\right) \tag{48}$$

$$P^L_{h_s^\pm} - P^L_0 = \pi + \frac{1}{2}\left[(-\pi + \Delta/2) + (\pi - \Delta/2)\right] = \pi \quad . \tag{49}$$

This gives $h_s^+ = h_s^- = 1/4$, and $P^\infty_{h_s} = \pi$.

3. Correlation functions at large times and distances

a. $n<1$ or ($n=1$ and $U/W<1$): According to the results in the last subsection and the general formulae from conformal field theory (38) we are now in position to deduce the long-range behavior of correlation functions:

$$C^{\mathrm{SS}}(x,t) \sim A\left(\frac{1}{x-v_s^R t}\right)^2 \tag{50a}$$

$$C^{\mathrm{NN}}(x,t) \sim B\left(\frac{1}{x+|v_c^L|t}\right)^2 \tag{50b}$$

$$G_\sigma(x,t) \sim \frac{e^{-ik_F^e x}}{2\pi}\frac{1}{\sqrt{(x-v_s^R t)+i/\Lambda_t}}\frac{1}{\sqrt{(x+|v_c^L|t)+i/\Lambda_t}} \tag{50c}$$

where Λ_t is a cut-off parameter ($\Lambda_t = \Lambda \mathrm{sgn} t$).

Note that the two-particle correlation functions are of the Fermi Liquid form, with renormalized velocities. On the other hand, the one-particle Green's function displays Luttinger Liquid behavior involving square-root singularities rather than the conventional quasiparticle asymptotic form, $1/\left(x-v_F t\right)$. Consequently, the Fourier transformed one-particle Green's function shows *no* quasiparticle peak, i.e., there is no contribution proportional to $\delta(\omega - v_F k)$ in the one-particle spectral function.

In fact, the form of $G_\sigma(\omega,k)$ is very interesting but rather complicated. A detailed analysis of its properties was given recently in refs. 37,38. Nevertheless, we can already see by dimensional analysis that there is a step-discontinuity in the momentum distribution $n_{k,\sigma} = \langle \hat{c}^+_{k,\sigma}\hat{c}_{k,\sigma}\rangle = (-i)\sum_r \exp(ikr)G(r,t=0_-)$ at $k=k_F^e=\pi(n-1)$. Our model provides a novel example of a system which displays a discontinuity in $n_{k,\sigma}$ in the absence of single-electron like quasi-particle excitations. Such systems have been termed "free Luttinger Liquids"[16] or "Gutzwiller Liquids"[1]. This unusual behavior would reflect itself, for example, in the dependence of the Kondo-temperature on the Kondo coupling impurity embedded in a "Gutzwiller Liquid"[39].

b. $n=1$ and $U/W>1$: The charge-charge correlation function and the one-particle Green's function decay exponentially, while the spin-spin correlation function has the asymptotic behavior

$$C^{\mathrm{SS}}(x,t) \sim A_1 \left(\frac{1}{x - v_s^R t}\right)^2 + A_2 \left(\frac{1}{x + |v_s^L| t}\right)^2 + A_3 \frac{\exp{(i\pi x)}}{\sqrt{(x - v_s^R t)\,(x + |v_s^L| t)}} \quad . \tag{51}$$

Due to the mixture of right- and left-moving spinons, an additional structure ("$2k_F$-oscillations") appears in $C^{\mathrm{SS}}(x,t)$, indicating strong antiferromagnetic correlations beyond the MCIT.

4. Equal-time correlation functions

Conformal field theory only allows us to calculate the long-range (large x *and* t) behavior of correlation functions. On the other hand, the large x behavior at $t = 0$, involves contributions from *all* frequencies. From eqs. (50) it is already clear that the low-frequency modes lead to a $1/x^2$ decay for the equal-time spin-spin or density-density correlation function. What can be said about the high-frequency contributions?

a. $n < 1$ *or* $n = 1$ *and* $U/W < 1$*:* We know that there is a sharp cut-off wave vector for both charge- and spin-excitations. In particular, no spin-excitations are possible above $\mathcal{K}_F = \pi(2n-1)$. The highest momentum spin excitation of the ground state is

$$\text{maximum } Q \text{ spin-exc.:} \quad \sigma[\uparrow\downarrow]\ldots[\uparrow\downarrow]\sigma'\Big|_{\mathcal{K}_F} \circ \ldots \circ$$

with $Q = \pi + [(\mathcal{K}_F - \Delta/2) + (-\pi + \Delta/2)]/2 = n\pi$. This corresponds to a sharp edge in the correlation function as a function of momentum q at $q = Q$ (for $n < 1$ or $n = 1$ and $U/W < 1$ the correlation functions do not diverge at $q = Q$). As in ordinary Fermi Liquids, this reflects itself in long-range oscillations in real space: $C^{\mathrm{SS}}(r, t=0) \sim A_1/r^2 + A_2 \cos(\pi n r)/r^2$. The same argument applies to the $t = 0$ density-density correlation function which also shows long-range $2k_F$-oscillations[3]. Finally, the single-particle momentum distribution shows step discontinuities at both ends of the $U = 0$ Fermi "surface".

b. $n = 1$ *and* $U/W > 1$*:* In this regime, the entire large distance behavior is already contained in the large momentum-transfer modes which are also gapless. More explicitly, for large r we find

$$C^{\mathrm{SS}}(r) \sim A_1 \frac{(-1)^r}{r} + A_2 \frac{1}{r^2} \tag{52}$$

which shows strong antiferromagnetic correlations above the MCIT. The slow oscillating decay of $C^{\mathrm{SS}}(r)$ corresponds to a logarithmic divergence of the spin-spin correlation function in momentum space near $q = \pi$.

B. 1/r-tJ model

1. Conformal Charge

As expected, eq. (31) implies $c = 1$[35]. Note that the formulae (36) cannot be applied exactly at the MSIT, $J = J_c$. At the transition we have *both* gapless right-moving spin-excitations *and* gapless right- and left-moving charge-excitations with *finite* velocities $v_s^R = J_c\pi/2$, $v_c^R = -v_c^L = J_c\pi n/2$. Nevertheless, the correct form of the $1/L$ correction at $J = J_c$, $\left[E_0^L - L\epsilon_0\right](J = J_c) = -\left[\pi/(6L)\right]\pi n J_c$, does not contain a contribution from all these three gapless excitations. Rather, since a finite density of spin-excitations produces an effective gap for the charge excitations and vice versa, only one of the two excitations, spin or charge, should be taken into account at $J = J_c$. More precisely, the factor, $\pi n J_c$ in the $1/L$ correction to the energy can be written in either of two forms, $\pi n J_c = v_s^R(J \to J_c^-) + |v_c^L(J \to J_c^-)| - |v_c^L(J = 0)|$ (for the origin of the term $v_c^L(J = 0)$ see the discussion for the $1/r$-Hubbard model, eq. (41)), or $\pi n J_c = v_c^R(J \to J_c^+) + |v_c^L(J \to J_c^+)|$. In other words, the correct value of the $1/L$ corrections is obtained by taking the limit from either above or below the transition.

2. Conformal dimensions

a. $J < J_c$: We can again use all results from the $1/r$-Hubbard model in the limit of large U/W. For two-particle excitations we then obtain $h_s^+ = 1$, $P_{h_s^+}^\infty = 0$; $h_c^- = 1$, $P_{h_c^-}^\infty = 0$. Note that for half-filling we have additional excitations which give $h_s^\pm = 1/4$, $P_{h_s^\pm}^\infty = \pi$. For the one-particle excitations all excitations involving charges at gaped for $n = 1$, while for $n < 1$ we have $h^c_N = h^s_N = 1/4$, $P^\infty_N = \pi(n-1) = k^e_F$.

b. $J > J_c$: Since above the transition we have no gapless spin excitations, all correlation functions involving spin excitations (spin-spin correlation function, one-particle Green's function) decay exponentially. On the other hand, we have additional charge excitations: besides the right-moving holon near $\mathcal{K}_1$ ($h^+_c = 1$, $P^\infty_{h^+_c} = 0$) we also find a left-moving holon near $\mathcal{K}_2$ ($h^-_c = 1$, $P^\infty_{h^-_c} = 0$). Furthermore, we can have a left-moving holon near $\mathcal{K}_1$ and a right-moving holon near $\mathcal{K}_2$. These excitations obey $h^\pm_c = 1/2$, $P^\infty_{h^\pm_c} = \pm(\mathcal{K}_2 - \mathcal{K}_1) = \pm 2\pi n$.

3. Correlation functions at large times and distances

For $J < J_c$ we obtain the same results as for the Hubbard model away from the transition, while $J > J_c$ both the spin-spin correlation function and the one-particle Green's function decay exponentially. On the other hand, the charge-charge correlation function behaves asymptotically like ($v_c = v^R_c = -v^L_c = J\pi n/2$)

$$C^{\rm NN}(x,t) \sim B_1 \left[\left(\frac{1}{x - v_c t} \right)^2 + \left(\frac{1}{x + v_c t} \right)^2 \right] + B_2 \left[\frac{\exp{(i2\pi n x)}}{(x - v_c t)} + \frac{\exp{(-i2\pi n x)}}{(x + v_c t)} \right] \quad . \tag{53}$$

Note that since in this case large momentum-transfer excitations are also gapless, $C^{\rm NN}(x,t)$ displays "$4k_F$-oscillations"[3].

4. Equal-time correlation functions

For $J < J_c$ we know that the exact wave function is the Gutzwiller-projected Fermi-sea, in which case all ground state correlation functions are explicitly known[21,40] for all densities n and distances r. In particular[21],

$$C^{\rm SS}(r \neq 0) = \frac{(-1)^r}{\pi r} \left[{\rm Si}\,(\pi r) - {\rm Si}\,(\pi r\,(1-n)) \right] \tag{54}$$

where ${\rm Si}(x) = \int_0^x dt \sin t / t$ is the sine-integral. At half-filling, the asymptotic behavior[21], $C^{\rm SS}(r \gtrsim 5) \simeq (-1)^r/(2r)$, reflects the strong antiferromagnetic correlations. The formulae for the density-density correlation function are rather involved but they show the expected large-distance behavior

$$C^{\mathrm{NN}}(r) \sim \frac{B_1}{r^2} + \frac{B_2}{r^2}\cos(\pi n r) + \frac{B_3}{r^4}\cos(2\pi n r) \quad . \tag{55}$$

The momentum distribution is found to have a jump discontinuity[40] of size $n_{k^e_{F,+}} - n_{k^e_{F,-}} = \sqrt{1-n}$. It is comforting that all general considerations from conformal field theory are verified in a limit where a complete description of the ground state properties is available.

For $J > J_c$, both spin-spin correlation function and the one-particle Green's function decay exponentially. The large momentum transfer processes for the density-density correlation function are no longer gaped and the large distance behavior even at $t = 0$ can be deduced from conformal field theory. We find

$$C^{\mathrm{NN}}(r) \sim 2B_1\frac{1}{r^2} + 2B_2\frac{\cos 2\pi n r}{r} \quad . \tag{56}$$

The momentum transform of the density-density correlation function shows a logarithmic divergence at $q = 2\pi n$.

V. g-OLOGY APPROACH AND CHARGE TRANSPORT PROPERTIES IN THE 1/r-HUBBARD MODEL

At low energies/temperatures normal electronic systems in one dimension can be described by a continuum field theory[30]. The essential idea is to linearize the electron excitation spectrum near the two Fermi points, resulting in left- and right-moving fermions (momentum and/or energy transfer cutoffs Λ_B, Λ, must then be introduced to regularize integrals). These two species of fermions interact via several scattering channels characterized by coupling constants g_i, $i = 1, \ldots, 4$ which can also be spin-dependent ("g-ology" Hamiltonian). The two large momentum transfer processes are described by g_1, which parametrizes the scattering process which interchanges right- and left-moving particles ("backscattering"), and g_3, which represents the scattering of two left-moving particles into two right-moving particles and vice versa ("Umklapp-scattering"). The remaining processes, described by g_2 and g_4, involve a small momentum transfer, between a left-moving and a right-moving electron (g_2), and between electrons on the same branch (g_4). The model with g_2 and g_4 only is the Luttinger model[41] which has been solved exactly[42,30,16].

In general, there is no recipe to link the g-ology coupling constants to the parameters of a given lattice Hamiltonian without solving the lattice model exactly[14]. Moreover, this identification is only valid for interactions strengths smaller than the cutoff. In the case of the Hubbard model with cosine dispersion the Mott-Hubbard transition happens at half-filling for $U = 0_+$[43], so that the entire low-energy physics, including the physics of the transition, can be described within g-ology[14]. More generally, this approach is applicable to a wide class of one-dimensional electron systems, the so-called Luttinger Liquids, the low energy behavior of which is controlled by a weak coupling fixed point[16]. Below we will restrict ourselves to the discussion of the metallic phase ($n < 1$, or $n = 1$ and $U/W < 1$) of the $1/r$-Hubbard model, although a similar treatment can be also given for the metallic phase of the $t - J$ model.

A. Identification of the g-ology parameters

The $1/r$-Hubbard model is particularly simple as it describes only right-moving electrons which are, however, hopping *on a lattice*. It is thus immediately evident that, in the context of g-ology, the corresponding low-energy physics is described by a *pure* g_4*-model* ("chiral Luttinger model"), with a Hamiltonian

$$\hat{H}_{g_4} = \sum_{k,\sigma} (\hbar v_F k)\, \hat{a}^{+}_{k,\sigma} \hat{a}_{k,\sigma} + \frac{1}{L} \sum_{q} \frac{1}{2} \sum_{\sigma,\sigma'} g_4^{\sigma,\sigma'}\, \hat{\rho}_\sigma(q) \hat{\rho}_{\sigma'}(-q) \quad . \tag{57}$$

Here, $\hat{\rho}_\sigma(q) = \sum_k \hat{a}^{+}_{k-q,\sigma} \hat{a}_{k,\sigma}$, the system volume (length of the ring) is $V = La$, $\hbar v_F \equiv ta$, and all terms of the Hamiltonian are understood to be normal ordered with respect to the ground state of the non-interacting Hamiltonian, $\hat{H}_0 = \hat{H}_{g_4 \equiv 0}$. The coupling matrix in (57) can be decomposed as $g_4^{\sigma,\sigma'} = g_4^{\parallel} \delta_{\sigma,\sigma'} + g_4^{\perp} \delta_{\sigma,-\sigma'}$. For sufficiently small values of U ($U/W << 1$) the lattice plays no role, and we may obviously identify $g_4^{\parallel} = \mathcal{O}(U^2)$, $g_4^{\perp} = U$.

After bosonization[16,30,42] the Hamiltonian (57) becomes *diagonal* in the new bosonic operators for charge ($\hat{\alpha}_k$) and spin ($\hat{\beta}_k$) and thus, the pure g_4-model is a "non-interacting" Luttinger Liquid or a "Gutzwiller Liquid"[1]. As discussed above, such a model does have a jump discontinuity in the momentum distribution although it is not a Fermi Liquid. The bosonic version of the g_4-Hamiltonian now reads

$$\hat{H}^c_{g4} = \sum_k (u_c k)\, \hat{\alpha}^+_k \hat{\alpha}_k \tag{58a}$$

$$\hat{H}^s_{g4} = \sum_k (u_s k)\, \hat{\beta}^+_k \hat{\beta}_k \,, \tag{58b}$$

with

$$|u_c| = v_F \left[1 + \frac{g^c_4}{2\pi\hbar v_F a^{-1}} \right] \tag{58c}$$

$$|u_s| = v_F \left[1 + \frac{g^s_4}{2\pi\hbar v_F a^{-1}} \right] \tag{58d}$$

$$g^c_4 = g^{\|}_4 + g^{\perp}_4 \tag{58e}$$

$$g^s_4 = g^{\|}_4 - g^{\perp}_4 \quad . \tag{58f}$$

To leading order in U/W, $g^c_4 = U = -g^s_4$, and thus, $|u_c| = v_F(1 + U/W)$, $|u_s| = v_F(1 - U/W)$[31]. Note that the lattice provides the natural cut-off parameters, $\Lambda = W$ and $\Lambda_B = \pi/a$.

It is amusing that, for our model, there is a way of extending the g-ology solution beyond the perturbative regime. In particular, by identifying the velocities, $|u_{c,s}|$, with the velocities of the charge and spin excitations found in our exact solution, eqs. (13), (7a), we can extract parameters $g^{c,s}_4$ for all values of U/W ($U/W \leq 1$ for $n = 1$). The resulting expressions read ($n = N/La$):

$$g^c_4 = U \frac{W}{\sqrt{(W+U)^2 - 4WUna}} > 0 \tag{59a}$$

$$g^s_4 = -U \frac{W}{U+W} < 0 \quad . \tag{59b}$$

For $na = 1$ (half-filling) $g^c_4 \to \infty$ for $U \to W_-$, reflecting the MCIT in the exact solution. The identification (59), for which we give a different argument in appendix C (for $n = 1$), allows us to follow the solution all the way to the MCIT by using the g-ology parametrization. This clarifies the fact that, in our model, the MCIT is not caused by the the relevance of g_3-processes at half-filling as in the Hubbard model with cosine dispersion (perfect nesting property), but rather, it arises as a pure renormalization of g_4^c due to the presence of the lattice.

B. Conductivity at zero temperature: Drude weight

In this section we make use of the g-ology approach to calculate the zero temperature Drude weight, D_c, of the zero-frequency peak of the real part of the conductivity,

$$\mathrm{Re}\left[\sigma(\omega)\right] = \mathcal{D}_c \delta(\omega) \quad \text{for} \quad \omega \to 0. \tag{60}$$

In the non-interacting limit, $\mathcal{D}_0 = e^2 t a^2/(\pi \hbar^2)$.

To obtain the electrical conductivity we start with the charge-charge Green's function ($\hat{\rho}(q) = \hat{\rho}_\uparrow(q) + \hat{\rho}_\downarrow(q)$ is the density operator in momentum space),

$$\chi^{\mathrm{NN}}(q,t) = \frac{-i}{La} \langle \mathcal{T} \hat{\rho}(q,t) \hat{\rho}(-q,0) \rangle \tag{61}$$

the retarded part of which is easily obtained from the g-ology analysis[30,44,14,32]:

$$\chi^{\mathrm{NN}}_{\mathrm{ret}}(q,\omega) = \frac{q}{\pi} \frac{1}{\omega - v_c^L q + i\eta}. \tag{62}$$

This form becomes exact for our model for small values of q and ω, and implies that the low-energy charge transport is entirely dominated by holons, eq. (10). As a check one may calculate the zero temperature compressibility as $\kappa(T=0) = \lim_{q\to 0} \lim_{\omega \to 0} \chi^{\mathrm{NN}}_{\mathrm{ret}}(q,\omega) = 1/\left(\pi |v_c^L|\right)$ in agreement with our direct calculation, eq. (15b).

Up to constant prefactors which we will put back in the end, the electrical conductivity follows from the generalized Einstein relation,

$$\sigma_{\mathrm{ret}}(q,\omega) = \frac{i\omega}{q^2} \chi^{\mathrm{NN}}_{\mathrm{ret}}(q,\omega), \tag{63}$$

which can be derived using the linear response formula for $\sigma_{\mathrm{ret}}(q,\omega)$ and the continuity equation, $-q\hat{j}(q,\omega)=\omega\hat{n}(q,\omega)$ (see also appendix D). The real part of the conductivity can then be calculated from $\mathrm{Re}\left[\sigma_{\mathrm{ret}}(q,\omega)\right]=|v_c^L|\delta(\omega-v_c^L q)$,

$$\sigma(\omega)=\lim_{q\to 0}\mathrm{Re}\left[\sigma_{\mathrm{ret}}(q,\omega)\right]=|v_c^L|\delta(\omega) \quad . \tag{64}$$

Adding back the constant prefactors gives then the final expression for the Drude weight

$$\mathcal{D}_c=\mathcal{D}_0\frac{|v_c^L|}{v_F}=\mathcal{D}_0\left[1+\frac{U}{\sqrt{(W+U)^2-4WUna}}\right] \quad . \tag{65}$$

Note that in our model the Drude weight *increases* with interaction. In fact, at half-filling, $\mathcal{D}_c$ is seen to *diverge* as $\sigma_{\mathrm{dc}}(\omega)=\sigma_0(\omega)/\left(1-U/W\right)$ for small ω and $U/W<1$. At the same time, the compressibility goes to zero, in such a way that the product, $\kappa\mathcal{D}_c$, remains constant. This behavior is in contrast to the MCIT observed in the Hubbard model with nearest-neighbor hopping, where, at finite U the MCIT can be approached from the metallic state by increasing the filling, $n\to 1^-$, $U>0$[14]. In that case, the compressibility *diverges* and the conductivity tends to zero.

In fact, it is clear that for any realistic dispersion the conductivity is bounded from above ("f-sum rule"[45,46]) and cannot diverge: $\int_{-\infty}^{\infty}d\omega\,\mathrm{Re}\sigma(\omega)\le F<\infty$. As shown in appendix D, F is finite whenever the bare dispersion $\epsilon(k)$ has a finite second derivative with respect to k everywhere. It is thus seen that it is our discontinuous dispersion relation $\epsilon(k)=t(k \bmod 2\pi)$ which allows for a diverging conductivity.

Finally, we note that since we do not know how a physical vector potential couples to the effective particles of our exact solution one cannot reliably determine the Drude weight by twisting the boundary conditions[47,46], corresponding to adding a flux, Φ, through the ring. In fact, if we naively replace all values $\mathcal{K}$ by $\mathcal{K}+\Phi/(La)$ to determine the ground state energy $E_0^L(\Phi)$, and try to evaluate

$$\mathcal{D}\overset{?}{=}\frac{e^2La}{\hbar^2}\left.\frac{\partial^2E_0^L(\Phi)}{\partial\Phi^2}\right|_{\Phi=0} \tag{66}$$

we would obtain the *incorrect* result for the Drude weight,

$$\begin{aligned}\mathcal{D} &= \mathcal{D}_0\left[\frac{v_s^R}{v_F} - 1 + \frac{|v_c^L|}{v_F} - 1\right] \\ &= \mathcal{D}_s + \mathcal{D}_c \quad ,\end{aligned} \tag{67}$$

which involves contributions from both charge *and* spin excitations.

VI. SUMMARY AND CONCLUSION

Above we discussed various aspects of the physics of two exactly solvable models of one dimensional lattice fermions: the $1/r$-Hubbard model and a related $1/r$-tJ model. The special feature of these models is that, due to absence of perfect nesting, they display non-trivial metal-to-charge-insulating and spin-insulating states, respectively, at a *finite* value of the coupling constants.

The $1/r$-Hubbard model thus provides for an explicit realization of Mott's and Hubbard's ideas[2,6] albeit in a rather pathological model in which the dispersion has a jump discontinuity at the zone boundaries. This peculiarity allows for a diverging Drude weight when the MCIT is approach from the metallic side, associated with the *vanishing* of the charge mass at the transition. While the behavior in the charge sector in the $1/r$-Hubbard model is rather non-generic, the spin sector reflects the expected physics of correlated Fermi systems: for example, the magnetic susceptibility strongly increases with interaction and develops a strong low-temperature peak at the spin-exchange energy scale $J = 4t^2/U$. After the MCIT the static spin-spin correlation function displays strong antiferromagnetic correlations with a logarithmic divergence in momentum space at $q = \pi$.

The $1/r$-tJ model with pair-hopping terms displays a metal-to-spin-insulator transition at $J_c = 4t/(\pi(1-n))$. The spin liquid state is described by the Gutzwiller projected Fermi-sea and provides an exactly solvable example of a genuine RVB-state. At the MSIT, simultaneously with the opening of a spin gap, the zero-frequency "spin-conductivity" (Drude weight for spin transport) drops to zero, after having increased with J/t (to a finite value) on the spin liquid side. The MSIT appears as a pure level-crossing effect, and thus should not be interpreted as a Mott-type transition[6].

We also found that, with a few changes related to the high symmetry of the spectrum in the non-interacting ($U = 0$ and $J = 0$) models, conformal field theory is applicable in the metallic and spin liquid states (i.e., away from transitions). Using conformal field theory and g-ology techniques allowed us to calculate long-distance/time properties of ground state correlation functions. The two-particle sector shows Fermi Liquid behavior. However, the single-particle Green's function does not lead to a quasi-particle peak in the spectral function, even though the jump discontinuity in the momentum distribution survives. Such systems are referred to as "free Luttinger Liquids" or "Gutzwiller Liquids". Within the g-ology approach the $1/r$-Hubbard model is identifyed as a "pure g_4-model" or "chiral Luttinger model". In our model the MCIT is driven by short distance lattice effects which lead to a divergence of the interaction parameter g_4^c at the MCIT.

Despite their conceptual shortcomings the two models provide instructive examples for strongly correlated electron systems. Although a rigorous proof is still missing we think that our models and results can be used to check the capability of numerical techniques and the applicability of various approximations[48].

ACKNOWLEDGMENTS

F.G. would like to thank his colleagues at Rutgers University for their hospitality during a visit, and the Deutsche Forschungsgemeinschaft (DFG) for traveling funds. This research was supported in part by a grant from the U.S. Department of Energy, Office of Basic Energy Sciences, Division of Materials Research (D.L.C.), and by ONR Grant # N00014-92-J-1378 and a Sloan Foundation Fellowship (A.E.R.).

APPENDIX A: CALCULATION OF GROUND STATE PROPERTIES IN THE PRESENCE OF A MAGNETIC FIELD

In this appendix we calculate some ground state properties in the presence of a weak magnetic field $\mathcal{H}_0$, and will eventually let $\mathcal{H}_0 \to 0$.

1. 1/r-Hubbard Model

In the presence of a magnetic field we will have a finite magnetization. Spin pairs will be broken and turned into the direction of the magnetic field. The positions of these unpaired spins is determined by the spinon dispersion (6). From the discussion above and figure 1 it is clear that they will always be located around $\mathcal{K} = -\pi$. For $n = 1$ and $U/W > 1$ there are also some upturned spins around $\mathcal{K} = \pi$. We exemplify the calculation for the latter case.

For $n = 1$, $U/W > 1$, and $m > 0$ the ground state is represented by

$$\text{ground state:} \quad \uparrow \ldots \uparrow\Big|_{\mathcal{K}_1} [\uparrow\downarrow] \ldots [\uparrow\downarrow]\Big|_{\mathcal{K}_2} \uparrow \ldots \uparrow$$

where the magnetization m is given by $\mathcal{K}_1 - \mathcal{K}_2 = 2\pi(m-1)$. The ground state energy density is calculated as $e_0(n = 1, \mathcal{K}_1, \mathcal{K}_2) = (1/2\pi) \int_{\mathcal{K}_1}^{\mathcal{K}_2} d\mathcal{K}\, [J(\mathcal{K})/2]$ where the additional factor 1/2 took into account that only every second $\mathcal{K}$ value contributes to the integral. We are only interested in small fields and expand $\mathcal{K}_{1,2} = \mp\pi(1 - \eta_{1,2})$ with $\eta_{1,2} \ll 1$. To second order we then obtain with the help of eqs. (5), (7a), and (7b)

$$e_0(\eta_1, \eta_2, n = 1) = e_0(n = 1) + \frac{\pi}{8}\left(\eta_1^2 v_s^R + \eta_2^2 |v_s^L|\right) \quad . \tag{A1}$$

Using $m = (\eta_1 + \eta_2)/2$ we minimize $e_0(n = 1, \eta_1, \eta_2) - m\mathcal{H}_0$ with respect to $\eta_{1,2}$, and obtain $\eta_{1,2} = (2\mathcal{H}_0)/(\pi|v_s^{L,R}|)$. The magnetization becomes

$$m = \mathcal{H}_0\left(\left(\pi v_s^R\right)^{-1} + \left(\pi|v_s^L|\right)^{-1}\right) = \frac{4\mathcal{H}_0 U}{W^2} \tag{A2}$$

and the ground state energy reads

$$e_0(m \to 0, n = 1) = e_0(n = 1) + \frac{1}{8}\frac{W^2}{U}m^2 \quad . \tag{A3}$$

A similar calculation gives the ground state energy density for $n < 1$ or $n = 1$, $U/W < 1$ as

$$\begin{aligned} e_0(m, n < 1) = & \frac{U(n-m) - W\left[(1-n)n + (1-m)m\right]}{4} \\ & - \frac{1}{24WU}\left[\left((W+U)^2 - 4WUm\right)^{3/2} - \left((W+U)^2 - 4WUn\right)^{3/2}\right] \end{aligned} \qquad \text{(A4)}$$

which is valid for all m. Note that the limits $\mathcal{H}_0 \to 0$ and $n \to 1$ do not commute beyond the metal-to-insulator transition, just as in the usual Hubbard model[28].

2. 1/r-tJ Model

The ground state representation in the presence of a (not too big) magnetic field is given by

$$\text{ground state:} \quad {}_{-\pi}\Big| \uparrow \dots \uparrow \Big|_{\mathcal{K}_m} \circ \dots \circ \Big|_{\mathcal{K}_1} [\uparrow\downarrow] \dots [\uparrow\downarrow] \Big|_{\mathcal{K}_2} \circ \dots \circ \Big|_{\pi}$$

with $\mathcal{K}_2 - \mathcal{K}_1 = 2\pi(n-m)$ and $\mathcal{K}_m = \pi(2m-1)$. A straightforward integration gives $e_0(\mathcal{K}_1, \mathcal{K}_2, \mathcal{K}_m) = (-t/(4\pi))\left[\mathcal{K}_1^2 - \mathcal{K}_m^2 + \pi^2 - \mathcal{K}_2^2\right] - (J/(16\pi))\left[\pi^2(\mathcal{K}_2 - \mathcal{K}_1) - (\mathcal{K}_2^3 - \mathcal{K}_1^3)/3\right]$. We have to minimize $e_0(\mathcal{K}_1, \mathcal{K}_2, \mathcal{K}_m) - \mu n - \mathcal{H}_0 m$ with respect to $\mathcal{K}_1, \mathcal{K}_2, \mathcal{K}_m$, where we have to distinguish the cases (i) $\mathcal{K}_1 = \mathcal{K}_m$, and (ii) $\mathcal{K}_1 > \mathcal{K}_m$ to allow for a transition at some $J = J_c$.

(i) $\mathcal{K}_1 = \mathcal{K}_m$: we are below the transition, and we see that $\mathcal{K}_2 = \pi(2n-1)$, $\mathcal{K}_m = \pi(2m-1)$. In this case we can find the ground state energy density even without the minimization procedure. For small external fields it has the simple form

$$e_0(n, m, J < J_c) = -\frac{Wn(1-n)}{2} - \frac{J\pi^2(n-m)}{12}\left[3(n+m) - 2(n^2 + nm + m^2)\right] \quad . \qquad \text{(A5)}$$

By differentiating this expression with respect to m gives the connection between the external magnetic field $\mathcal{H}_0$ and the (small) magnetization density m

$$m = \mathcal{H}_0 \left(\pi v_s^R\right)^{-1} \quad . \qquad \text{(A6)}$$

(ii) $\mathcal{K}_1 > \mathcal{K}_m$: from the minimization equations one easily finds that $\mathcal{K}_1 + \mathcal{K}_2 = -4W/(\pi J)$. We thus get a solution

$$\mathcal{K}_1 > \mathcal{K}_m \quad , \quad \text{if} \quad J > J_c(m) = \frac{2W}{\pi^2(1-n-m)} \quad . \tag{A7}$$

Note that the presence of a magnetic field *stabilizes* the spin-liquid phase where spin-excitations are gapless: $J_c(m) > J_c(m=0) \equiv J_c$. The ground state energy density then reads

$$e_0(n,m,J > J_c(m)) = \frac{W^2}{2\pi^2 J}(n-m) - \frac{W}{2}m(1-m) - \frac{J\pi^2}{24}(n-m)\left[3-(n-m)^2\right] \quad . \tag{A8}$$

By differentiating this expression with respect to m gives the connection between the external magnetic field $\mathcal{H}_0$ and the (small) magnetization density m

$$\mathcal{H}_0 = \mathcal{H}_0^c + m\pi^2\left[J_c + n(J-J_c)\right] \tag{A9a}$$

$$\mathcal{H}_0^c = \frac{\pi^2(1-n)}{8}\left(1-\frac{J_c}{J}\right)\left[J(1+n) - J_c(1-n)\right] \quad . \tag{A9b}$$

It now takes a *finite* magnetic field $\mathcal{H}_0^c$ to magnetize the system. The spin gap is $\Delta\mu_s = 2\mathcal{H}_0^c$ (see (22)) because we break a pair of spins ($S=0$) to form an $S^z = S = 1$ state.

APPENDIX B: 1/L CORRECTIONS FOR THE GROUND STATE ENERGY OF THE 1/r-HUBBARD MODEL

The ground state energy for finite system sizes L (even) and a finite particle number N (even) is calculated for $n \leq 1$ as $E_0^L = -\sum'_{-\pi<\mathcal{K}<\mathcal{K}_F} J_{\mathcal{K}} + \sum_{\mathcal{K}_F<\mathcal{K}<\pi}(-t)\mathcal{K}$. The prime indicates that only every second of the $\mathcal{K} = \Delta(m+1/2)$ $m = -L/2, \ldots, L/2-1)$ has to be taken ($\mathcal{K}_F = \Delta(N-L/2)$). After rescaling $m = 2r - L/2 + 1$ the sums give

$$E_0^L = L\left[\frac{Un}{4} - \frac{Wn(1-n)}{4}\right] - \frac{1}{2}\sum_{r=0}^{N/2-1}\sqrt{W^2+U^2-4WU(2r+1)/L} \quad . \tag{B1}$$

To calculate the sum we use the Poisson sum formula (see, e.g., Ref. 49)

$$\sum_{r=0}^{N/2-1} h(r+1/2) = \int_0^{N/2} dx\, h(x) + 2\sum_{s=1}^{\infty}(-1)^s \int_0^{N/2} dx\, h(x)\cos(2\pi x s) \quad , \tag{B2}$$

do the first integral and a partial integration in the second, and arrive at

$$E_0^L - L\epsilon_0 = -\sum_{s=1}^{\infty}(-1)^s \frac{2WU}{L\pi s}\int_0^{N/2} dx \frac{\sin(2\pi x s)}{\sqrt{(W+U)^2 - 8WUx/L}} \quad . \tag{B3}$$

Away from $U = W$ and $n = 1$ we can do further and further partial integrations in the integral on the right hand side of this equation, and generate an expansion in $1/L$. Keeping only the first term gives

$$E_0^L - L\epsilon_0 = -\sum_{s=1}^{\infty}\frac{(-1)^s}{s^2}\frac{WU}{L\pi^2(W+U)}\left[1 - \frac{1}{\sqrt{1 - 4WUn/(W+U)^2}}\right] + \mathcal{O}\left(1/L^2\right) \quad . \tag{B4}$$

Doing the remaining sum and rearranging terms ($v_F = t = W/(2\pi)$ is the Fermi velocity) gives

$$E_0^L - L\epsilon_0 = \frac{\pi}{6L}v_F\left[\frac{U}{U+W} - \frac{U}{\sqrt{(W+U)^2 - 4WUn}}\right] \quad . \tag{B5}$$

With the help of eqs. (7) and (10) this can be cast into the form of eq. (41).

APPENDIX C: EFFECTIVE g_4-PARAMETERS AT HALF-FILLING FROM THE SCREENED ELECTRON-ELECTRON INTERACTION

There is a rather simple recipe to obtain $g_4^{c,s}$ for all $U/W < 1$ without referring to the exact solution. At half-filling we know that $k_F^e = 0$ lies symmetrically around the upper and lower band edge ($\pm W/2$ at $k = \pm\pi/a$). For a pure g_4-model one can exactly calculate the *screened* electron-electron interaction with the help of Ward-identities[30,44,32]. One finds

$$D_4^{c,s}(k,\omega) = g_4^{c,s}\frac{\omega - v_F k}{\omega - |u_{c,s}|k} \quad . \tag{C1}$$

The effective interaction integrated over all times is given by the $\omega = 0$ contribution which gives

$$D_4^{c,s}(k,0) = g_4^{c,s}\frac{v_F}{|u_{c,s}|} = g_4^{c,s}\frac{1}{1 + g_4^{c,s}/W} \quad . \tag{C2}$$

If we now *demand* that the time-integrated part of the screened interaction has to stay unrenormalized at its value for small U/W, $D_4^c(k,0) = U$ and $D_4^s(k,0) = -U$, we find that

$$g_4^c = U\frac{1}{1-U/W} \tag{C3a}$$

$$g_4^s = -U\frac{1}{1+U/W} \tag{C3b}$$

which is indeed the correct result. So far, we have not been able to obtain a general form for $g_4^{c,s}$ away from half-filling, without appealing to the exact solution.

APPENDIX D: f-SUM RULE FOR GENERAL DISPERSION RELATIONS

1. Current operator

For a Hamiltonian $\hat{H} = \hat{T} + \hat{V}$ we assume that the interaction only contains density operators $\hat{n}_r$. We omit spin indices in the following. The particle density operator $\hat{n}(q) = \sum_r e^{iqr}\hat{n}_r = \sum_k \hat{c}_{k+q}^{+}\hat{c}_k$ then commutes with $\hat{V}$. We expand the exponential in the particle density operator $\hat{n}(q)$ for small momenta q (this step could cause problems in the case of long-range hopping). The continuity equation then reads

$$i\frac{\partial}{\partial t}\hat{n}(q) = -q\sum_r \frac{\partial r}{\partial t}\hat{n}_r = -q\sum_r v(r)\hat{n}(r) \quad . \tag{D1}$$

The sum on the right-hand side is identified with the particle current operator

$$\hat{j} = \lim_{q\to 0}\frac{-i}{q}\frac{\partial}{\partial t}\hat{n}(q) \quad . \tag{D2}$$

Using the Heisenberg equations of motion we can calculate $\hat{j}$ as

$$\hat{j} = \lim_{q\to 0}\sum_k \hat{c}_{k+q}^{+}\hat{c}_k\left(\frac{\epsilon(k+q)-\epsilon(k)}{q}\right) \quad . \tag{D3}$$

If the dispersion relation is differentiable, this reduces to the standard expression for the current operator involving the group velocity $\partial\epsilon(k)/\partial k$. Our linear dispersion relation is not differentiable at $|k| = \pi$. Instead we may think that the linear dispersion relation is the result of a limiting process where we start with a differentiable dispersion $\widetilde{\epsilon}(k)$ which becomes ever steeper near $|k| = \pi$. This corresponds to ever faster left-moving electrons near $|k| = \pi$, in addition to the right-moving electrons for $|k| < \pi$. From this viewpoint it becomes clear that we have to expect a *singular* contribution from these "left-moving" electrons. Indeed, we find for $q > 0$

$$\hat{j}(q) = \frac{W}{2\pi} \sum_k \hat{c}^+_{k+q} \hat{c}_k - \frac{W}{q} \sum_{\pi - q < k < \pi} \hat{c}^+_{k+q} \hat{c}_k \tag{D4}$$

and $\hat{j}(-q) = \hat{j}^+(q)$. Now let $q \to 0$ and assume that we may approximately replace $\hat{c}^+_{k+q} \approx \hat{c}^+_k$. For the minimum $q = \Delta = 2\pi/L$ one has $\hat{j}(q = \Delta) = W/(2\pi) \left[\hat{N} - L \hat{c}^+_{-\pi+\Delta/2} \hat{c}_{\pi-\Delta/2}\right]$. As "the current at $q = 0$" one may *define*

$$\begin{aligned} \hat{j} &= \frac{1}{2} \left(\hat{j}(q = \Delta) + \hat{j}(q = -\Delta)\right) \\ &= W/(2\pi) \left[\hat{N} - (L/2) \left(\hat{c}^+_{-\pi+\Delta/2} \hat{c}_{\pi-\Delta/2} + \hat{c}^+_{\pi-\Delta/2} \hat{c}_{-\pi+\Delta/2}\right)\right] \quad . \end{aligned} \tag{D5}$$

We obviously get an extensive (i.e., singular) contribution from the states near the Brillouin zone boundary.

2. f-sum rule

We are interested in the real part of the transverse conductivity for small q at temperature $T = 0$

$$\mathrm{Re}\left[\sigma(\omega, q \to 0)\right] = \frac{e^2}{L\omega} \lim_{q \to 0} \mathrm{Re} \left\{ \int_{-\infty}^{t} dt' e^{i\omega(t-t')} \langle \left[\hat{j}^+(q,t), \hat{j}(q,t')\right] \rangle \right\} \quad . \tag{D6}$$

Using the continuity equation (D1), the equation of motion (in t) (eq. (D3)), and integrating by parts (in t') one finds

$$\begin{aligned} \mathrm{Re}\left[\sigma(\omega, q \to 0)\right] = &-\frac{e^2}{L\omega q^2} \mathrm{Re} \Big\{ (-i) \, \langle \left[\left[\hat{\rho}^+(q,t), \hat{T}\right], \hat{\rho}(q,t')\right] \rangle e^{i\omega(t-t')} \Big|_{-\infty}^{t} \\ &-(-i)(-i\omega) \int_{-\infty}^{t} dt' e^{i\omega(t-t')} \langle \left[\left[\hat{\rho}^+(q,t), \hat{T}\right], \hat{\rho}(q,t')\right] \rangle \Big\} \, . \end{aligned} \tag{D7}$$

The first term in $\{\ldots\}$ is purely imaginary and drops out. To obtain the f-sum rule we integrate over all ω. This gives

$$\begin{aligned} F(q) &\equiv \int_{-\infty}^{\infty} d\omega \mathrm{Re}\left[\sigma(\omega, q \to 0)\right] \\ &= -\frac{\pi e^2}{L q^2} \langle \left[\left[\hat{\rho}^+(q), \hat{T}\right], \hat{\rho}(q)\right] \rangle \end{aligned} \tag{D8}$$

because the expression (D7) only depended on $(t - t')$. The double commutator gives

$$\left[\left[\hat{\rho}^{+}(q), \hat{T}\right], \hat{\rho}(q)\right] = \sum_{k} \hat{c}_{k}^{+} \hat{c}_{k} \left[\epsilon(k) - \epsilon(k+q) + \epsilon(k) - \epsilon(k-q)\right]$$

Thus,

$$F(q) = \frac{\pi e^2}{L} \sum_{k} \left\{ \frac{1}{q} \left[\frac{\epsilon(k+q) - \epsilon(k)}{q} + \frac{\epsilon(k-q) - \epsilon(k)}{q} \right] \right\} \langle \hat{n}_k \rangle \tag{D9}$$

and $F = \lim_{q \to 0} F(q)$. For twice differentiable dispersion relations this reduces to $F = (\pi e^2/L) \sum_k \langle \hat{n}_k \rangle \left[\partial^2 \epsilon(k)/\partial k^2\right]$. In particular, for a cosine dispersion, $F = \pi e^2 \langle -\hat{T} \rangle / L$ which is the standard result[45,46].

For the linear dispersion we get

$$F(q) = \frac{\pi e^2 W}{L q^2} \left\{ \sum_{-\pi < k < -\pi + q} \langle \hat{n}_k \rangle - \sum_{\pi - q < k < \pi} \langle \hat{n}_k \rangle \right\} \quad . \tag{D10}$$

The minimum value of q is $\Delta = 2\pi/L$. Thus

$$F \equiv F(\Delta) = L \frac{e^2}{4\pi} \left[\langle \hat{n}_{\pi - \Delta/2} \rangle - \langle \hat{n}_{-\pi + \Delta/2} \rangle \right] \quad . \tag{D11}$$

The f-sum rule is thus *extensive* and leaves room for a diverging Drude weight. This can only happen, if the dispersion relation $\epsilon(k)$ is not twice differentiable with respect to k.

REFERENCES

[1] F. Gebhard and A.E. Ruckenstein, Phys. Rev. Lett. **68**, 244 (1992).

[2] J. Hubbard, Proc. R. Soc. London, Ser. A **276**, 238 (1963).

[3] The diameter of the Fermi body is πn as usual. This is the wave vector that enters in the long distance behavior of correlation functions, and is identified with "$\pi n = 2k_F$".

[4] P.W. Anderson in *Solid State Physics*, ed. by F. Seitz and D. Turnbull, vol. **14**, p. 99 (1963); J.E. Schrieffer and P.A. Wolff, Phys. Rev. **149**, 491 (1966); A.B. Harris and R.V. Lange, Phys. Rev. **157**, 295 (1967).

[5] F.D.M. Haldane, Phys. Rev. Lett. **60**, 635 (1992); B.S. Shastry, Phys. Rev. Lett. **60**, 639 (1992).

[6] N.F. Mott, Rev. Mod. Phys. **40**, 677 (1968); *Metal-Insulator Transitions*, (Taylor & Francis, London, 1974).

[7] P.W. Anderson, G. Baskaran, Z. Zou, and T. Hsu, Phys. Rev. Lett. **58**, 2790 (1987); F.C. Zhang and T.M. Rice, Phys. Rev. **B 37**, 3759 (1988); F.C. Zhang, C. Gros, T.M. Rice, and H. Shiba, Supercond. Sci. and Techn. **1**, 36 (1988).

[8] The configurations [●○] and [↑↓] represent charge ($C = C^z = 0$) and spin singlets ($S = S^z = 0$).

[9] D.F. Wang, Q.F. Zhang, and P. Coleman, (unpublished) (1993).

[10] P.W. Anderson, Science **235**, 1196 (1987).

[11] In a grand canonical ensemble we use $\hat{c}^+_{k,\sigma} \mapsto \hat{c}_{-k,-\sigma}$. The kinetic energy operator is invariant, and $\hat{D} - \sum_\sigma \mu_\sigma \hat{N}_\sigma \mapsto \hat{D} - \sum_\sigma \mu_\sigma \hat{N}_\sigma + (L - \sum_\sigma \hat{N}_\sigma)(U - \sum_\sigma \mu_\sigma)$. At half-filling this must be an operator identity so that we have to fix $\sum_\sigma \mu_\sigma = 2\mu = U$.

[12] W.F. Brinkman and T.M. Rice, Phys. Rev. **B 2**, 4302 (1970).

[13] D. Vollhardt, Rev. Mod. Phys. **56**, 99 (1984).

[14] H.J. Schulz, Phys. Rev. Lett. **64**, 2831 (1990); Int. J. Mod. Phys. **B 5**, 57 (1991); *Proceedings of the Adriatico Research Conference and Miniworkshop on "Strongly Correlated Electron Systems II*, ed. by G. Baskaran et al. (Progress in High Temperature Superconductivity – Vol. 29, World Scientific, Singapore, 1991); C.F. Coll, Phys. Rev. **B 9**, 2150 (1974).

[15] H. Shiba and P.A. Pincus, Phys. Rev. **B 5**, 1966 (1972); H. Shiba, Prog. Theor. Phys. **48**, 2171 (1972); H. Shiba, Phys. Rev. **B 6**, 930 (1972).

[16] F.D.M. Haldane, J. Phys. C **14**, 2585 (1981); Phys. Rev. Lett. **45**, 1358 (1980); **47**, 1840 (1981).

[17] F.D.M. Haldane, Phys. Rev. Lett. **66**, 1529 (1991).

[18] J. des Cloizeux and J.J. Pearson, Phys. Rev. **128**, 2131 (1962).

[19] The unique ground state at $U = 0$ (Fermi sea) and for $U > 0$ contain one and the same configuration with no double occupancy. It is the only one to survive for $U \to \infty$, hence the Gutzwiller projected Fermi sea is the exact ground state for the $1/r$-tJ model at all fillings.

[20] H. Yokoyama and H. Shiba, J. Phys. Jpn. **56**, 1490 (1987); *ibid.* 3570 (1987); *ibid.* 3582 (1987); *ibid.* **57**, 2482 (1988); C. Gros, R. Joynt, and T.M. Rice, Phys. Rev. **B 36**, 381 (1987); C. Gros, Phys. Rev. **B 38**, 931 (1988).

[21] F. Gebhard and D. Vollhardt, Phys. Rev. Lett. **59**, 1472 (1987); Phys. Rev. **B 38**, 6911 (1988).

[22] H. Yokoyama and M. Ogata, Phys. Rev. Lett. **67**, 3610 (1991).

[23] J. Ashkin and E. Teller, Phys. Rev. **64**, 178 (1943).

[24] L. Onsager, Phys. Rev. **65**, 117 (1944); see also R.J. Baxter, *Exactly solved models in*

statistical mechanics, (Academic Press, New York, 1982).

[25] There is always a true gap between $\lambda_{\mathcal{K}}^{-}$ and $\lambda_{\mathcal{K}}^{+}$ so that the contribution of the $\lambda_{\mathcal{K}}^{-}$ to the free energy density does not show up in a $1/L$-expansion.

[26] A. A. Belavin, A.M. Polyakov, and A.B. Zamolodchikov, Nucl. Phys. **B 241**, 333 (1984).

[27] J.L. Cardy, Nucl. Phys. **B 270** [FS16], 186 (1986); H.W. Blöte, J.L. Cardy, and M.P. Nightingale, Phys. Rev. Lett. **56**, 742 (1986); A.D. Mirnov and A.V. Zabrodin, Phys. Rev. Lett. **66**, 534 (1991).

[28] H. Frahm and V.E. Korepin, Phys. Rev. **B 42**, 10553 (1990); **B 43**, 5653 (1991).

[29] N. Kawakami and S.-K. Yang, Phys. Lett. **148A**, 359 (1990); Phys. Rev. Lett. **65**, 2309 (1990); Prog. Theor. Phys. Suppl. **107**, 59 (1992).

[30] J. Sólyom, Adv. Phys. **28**, 201 (1979).

[31] J. Voit, Phys. Rev. **B 45**, 4027 (1992).

[32] W. Metzner and C. di Castro, Phys. Rev. **B 47**, 16107 (1993).

[33] J. Carmelo and A.A. Ovchinnikov, J. Phys. **C 3**, 757 (1991); J.M.P. Carmelo, P. Horsch, and A.A. Ovchinnikov, Phys. Rev. **B 45**, 7899 (1992); J.M.P. Carmelo and P. Horsch, Phys. Rev. Lett. **68**, 871 (1992).

[34] I. Affleck, Phys. Rev. Lett. **56**, 746 (1986).

[35] Note that our model is chiral, i.e., the density of states is only half as big as in the usual case.

[36] G. Albertini, B.M. McCoy, J.H.H. Perk, S. Tang, Nucl. Phys. **B 314**, 741 (1989); R.J. Baxter, J. Stat. Phys. **57**, p. 1 (1989).

[37] V. Meden and K. Schönhammer, Phys. Rev. **B 46**, 15753 (1992), and unpublished (1993).

[38] J. Voit, Phys. Rev. **B 47**, 6740 (1993), and unpublished (1993).

[39] D.-H. Lee and J. Toner, Phys. Rev. Lett. **69**, 3378 (1992), and private communication.

[40] W. Metzner and D. Vollhardt, Phys. Rev. Lett. **59**, 121 (1987); Phys. Rev. **B 37**, 7382 (1988).

[41] J.M. Luttinger, J. Math. Phys. **4**, 1154 (1963).

[42] D.C. Mattis and E.H. Lieb, J. Math. Phys. **6**, 304 (1965).

[43] E.H. Lieb and F.Y. Wu, Phys. Rev. Lett. **20**, 1445 (1968).

[44] E.H. Rezayi, J. Sak, and J. Sólyom, Phys. Rev. **B 20**, 1129 (1979); *ibid.* **B 23**, 1342 (1981); K. Penc and J. Sólyom, Phys. Rev. **B 44**, 12690 (1991).

[45] See, e.g., D. Pines and P. Nozières, *Theory of Quantum Liquids* (Benjamin, New York, 1966); P.F. Maldague, Phys. Rev. **B 16**, 2437 (1977).

[46] B.S. Shastry and B. Sutherland, Phys. Rev. Lett. **65**, 243 (1990).

[47] W. Kohn, Phys. Rev. **133**, A 171 (1964); for recent applications, see C.A. Stafford, A.J. Millis, and B.S. Shastry, Phys. Rev. **B 43**, 13660 (1991); R.M. Fye, M.J. Martins, D.J. Scalapino, J. Wagner, and W. Hanke, Phys. Rev. **B 45**, 7311 (1992).

[48] F. Gebhard and A. Girndt, "Comparison of Variational Approaches for the Exactly Solvable $1/r$-Hubbard model", available as preprint cond-mat/9307036 from the preprint library `cond-mat@babbage.sissa.it` (accepted for publication in Z. Phys. B).

[49] L.D. Landau and E.M. Lifshits, *Statistical Physics, part 1*, Course on Theoretical Physics Vol. V, § 60 (3rd edition, Pergamon Press, New York, 1980).

FIGURES

FIG. 1. Dispersion relations for (a) spinons, see eq. (6), and (b) chargeons, see eq. (9), in the $1/r$-Hubbard model for (a) $U/W = 0.25, 0.5, 0.75, 1, 2,$ and (b) $U/W = 0.5, 1, 2$.

FIG. 2. Total density of states (a) D_s of the spinons and (b) D_c of the chargeons for the U/W-values of fig. 1 in the $1/r$-Hubbard model (note the change in energy scale); the energy gap in D_c for $U > W$ is only half as big as the true gap because the chargeons always come in *pairs*.

FIG. 3. Specific heat as a function of temperature for the half-filled $1/r$-Hubbard model for various values of U/W (a) below ($U/W = 0, 0.5, 0.75, 1$), (b) above ($U/W = 1, 2, 4$) the metal-to-charge-insulator transition.

FIG. 4. Fluctuation of the particle density $k_B T \kappa(n = 1, T)$ for the half-filled $1/r$-Hubbard model as a function of temperature for $U/W = 0, 0.5, 1, 2$.

FIG. 5. Magnetic susceptibility $\chi(n = 1, T)$ for the half-filled $1/r$-Hubbard model as a function of temperature for $U/W = 0, 0.5, 1, 2$.

FIG. 6. Chemical potential $\mu(n = 0.75, T)$ in the $1/r$-tJ model as a function of temperature for $J/J_c = 0.5, 0.99, 1.02, 1.2, 2$; the metal-to-spin-insulator transition happens at $J_c = 0.81W$.

FIG. 7. Specific heat $c_v(n = 0.75, T)$ in the $1/r$-tJ model as a function of temperature for $J/J_c = 0.49, 0.99, 1.02, 2.47$.

FIG. 8. Sommerfeld coefficient $\gamma(n = 0.75, T)$ in the $1/r$-tJ model as a function of temperature for $J/J_c = 0.49, 0.99, 1.02, 2.47$.

FIG. 9. Compressibility $\kappa(n = 0.75, T)$ in the $1/r$-tJ model as a function of temperature (a) below ($J/J_c = 0.49, 0.74, 0.99$) and (b) above ($J/J_c = 1.02, 1.23, 1.73, 2.47$) the MSIT.

FIG. 10. Magnetic susceptibility $\chi(n = 0.75, T)$ in the $1/r$-tJ model as a function of temperature for $J/J_c = 0.49, 0.74, 0.99, 1.02, 1.23, 2.47$.

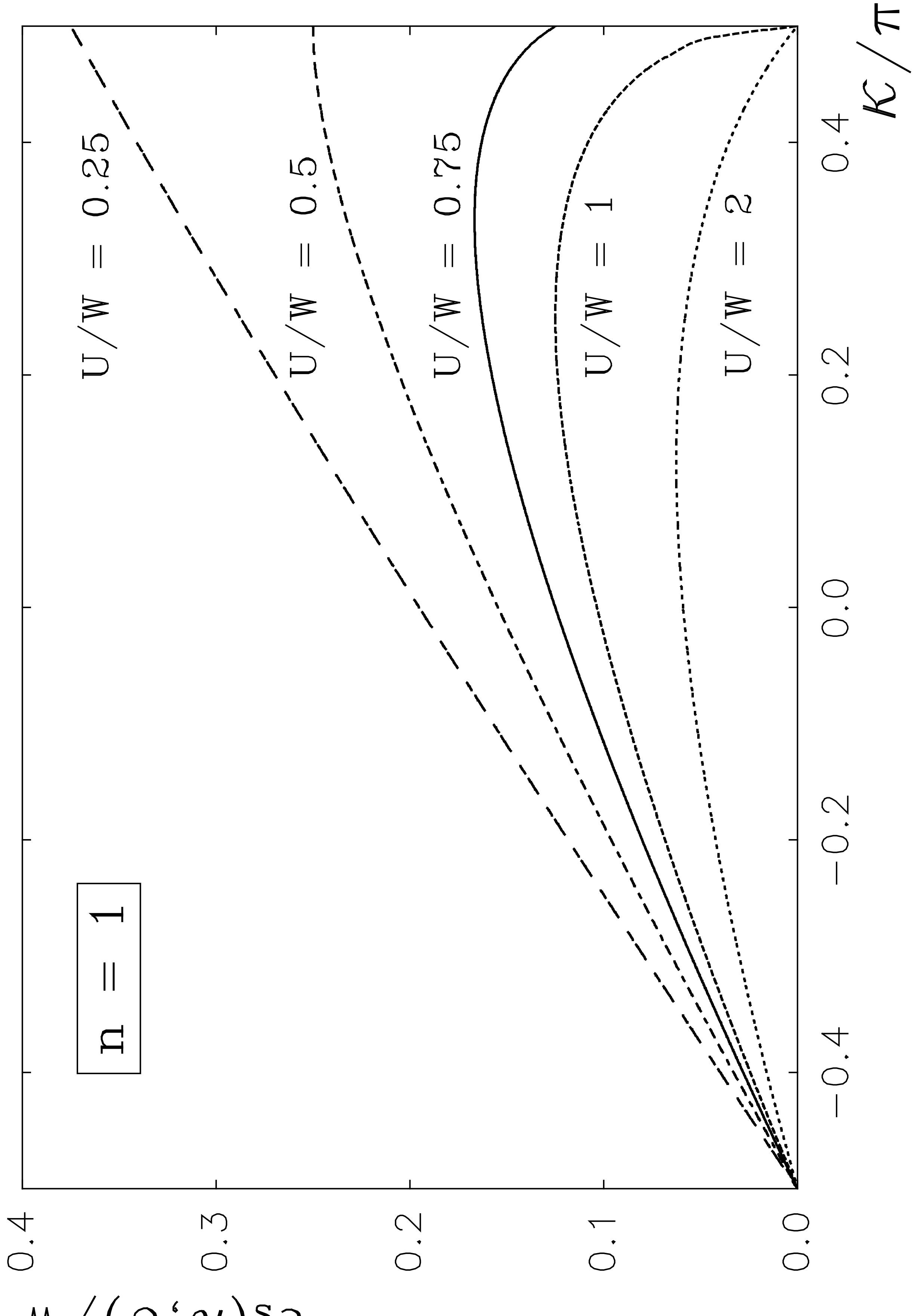
n = 1
U/W = 0.25
U/W = 0.5
U/W = 0.75
U/W = 1
U/W = 2
$\epsilon_s(\kappa,U)/W$
0.0
0.1
0.2
0.3
0.4
κ/π
−0.4
−0.2
0.0
0.2
0.4

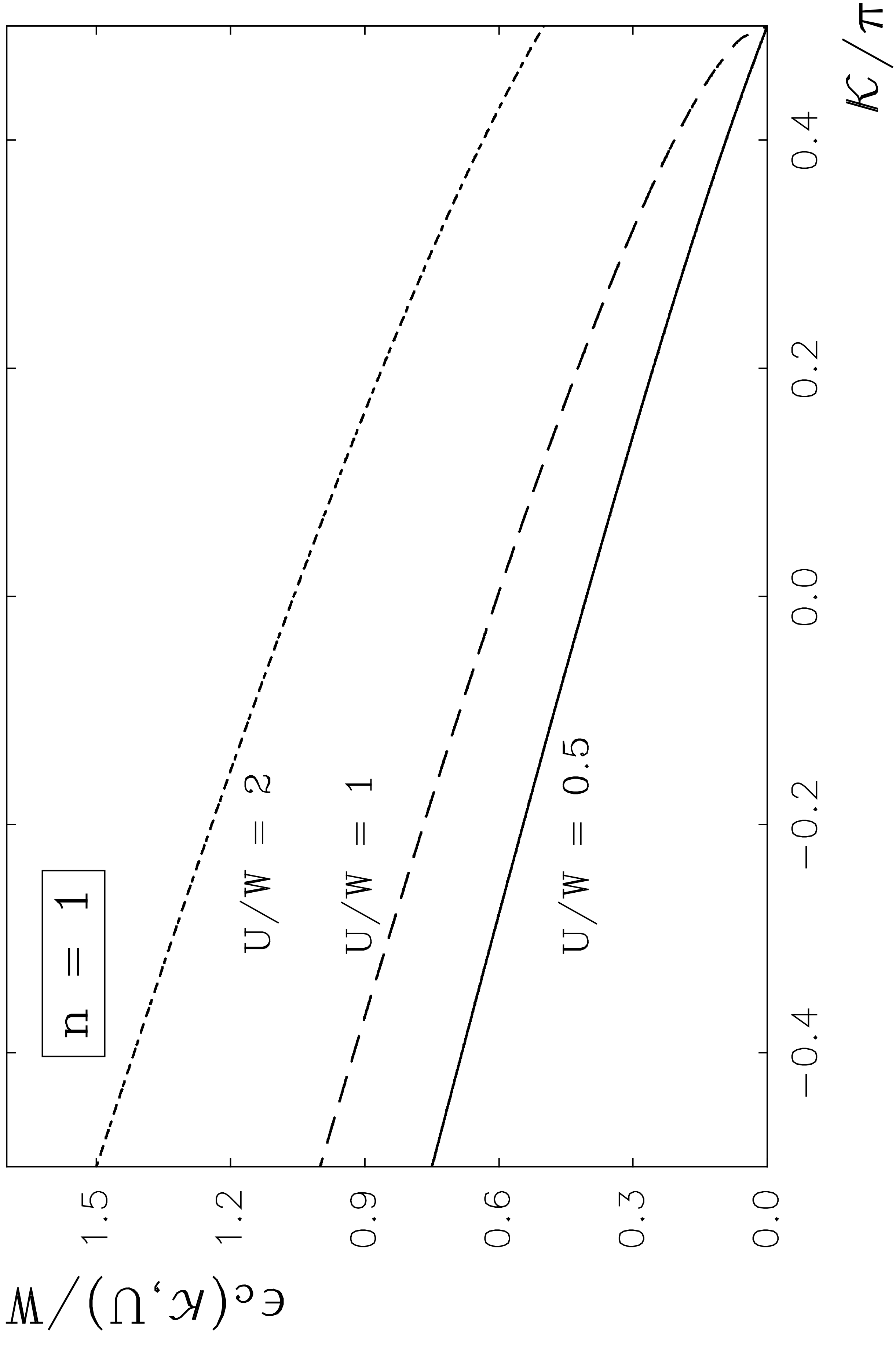

n = 1
U/W = 2
U/W = 1
U/W = 0.5
$\epsilon_c(\kappa, U)/W$
0.0
0.3
0.6
0.9
1.2
1.5
−0.4
−0.2
0.0
0.2
0.4
κ/π

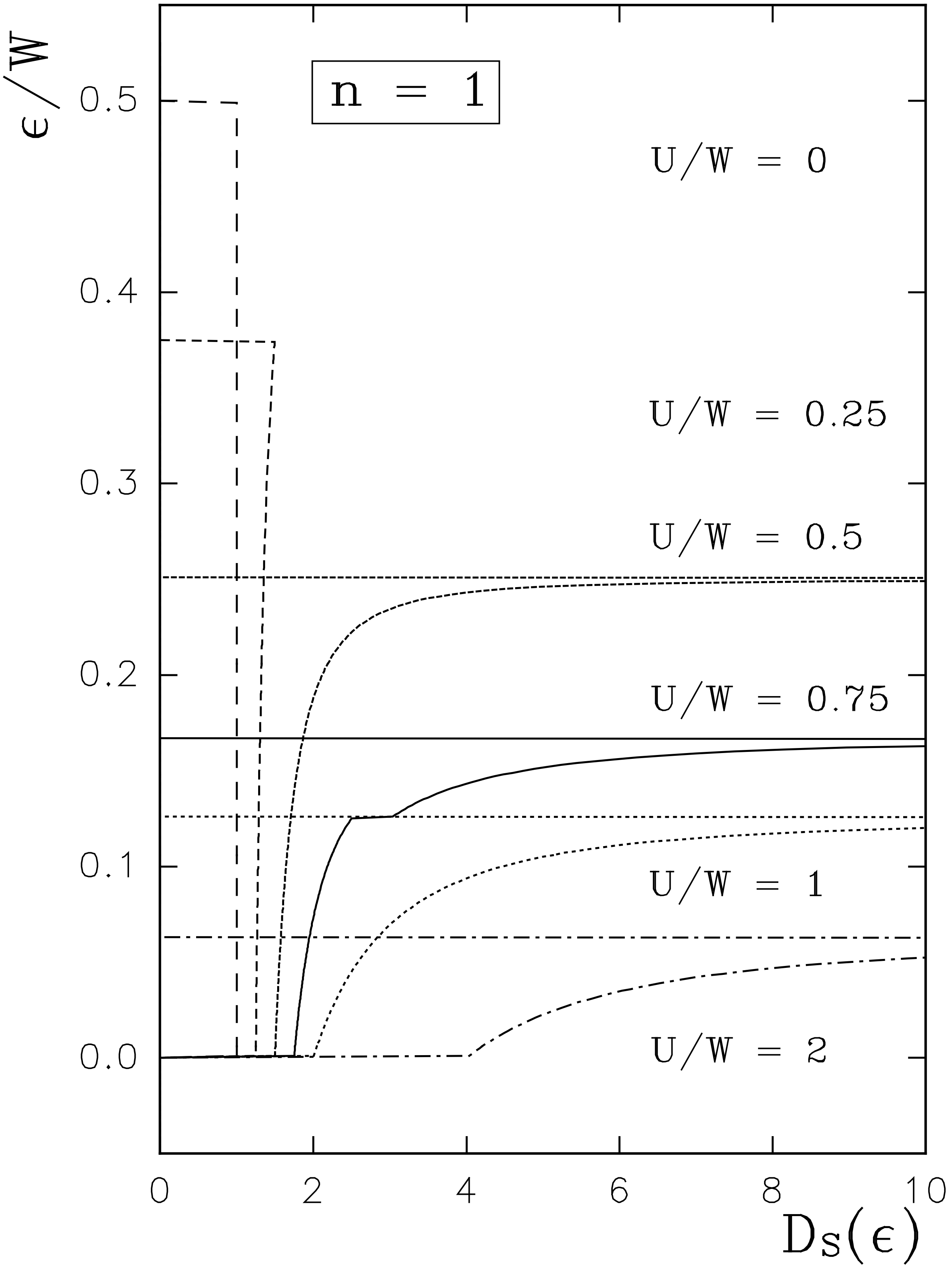
ε/W
n = 1
U/W = 0
U/W = 0.25
U/W = 0.5
U/W = 0.75
U/W = 1
U/W = 2
0.0
0.1
0.2
0.3
0.4
0.5
0
2
4
6
8
10
Ds(ε)

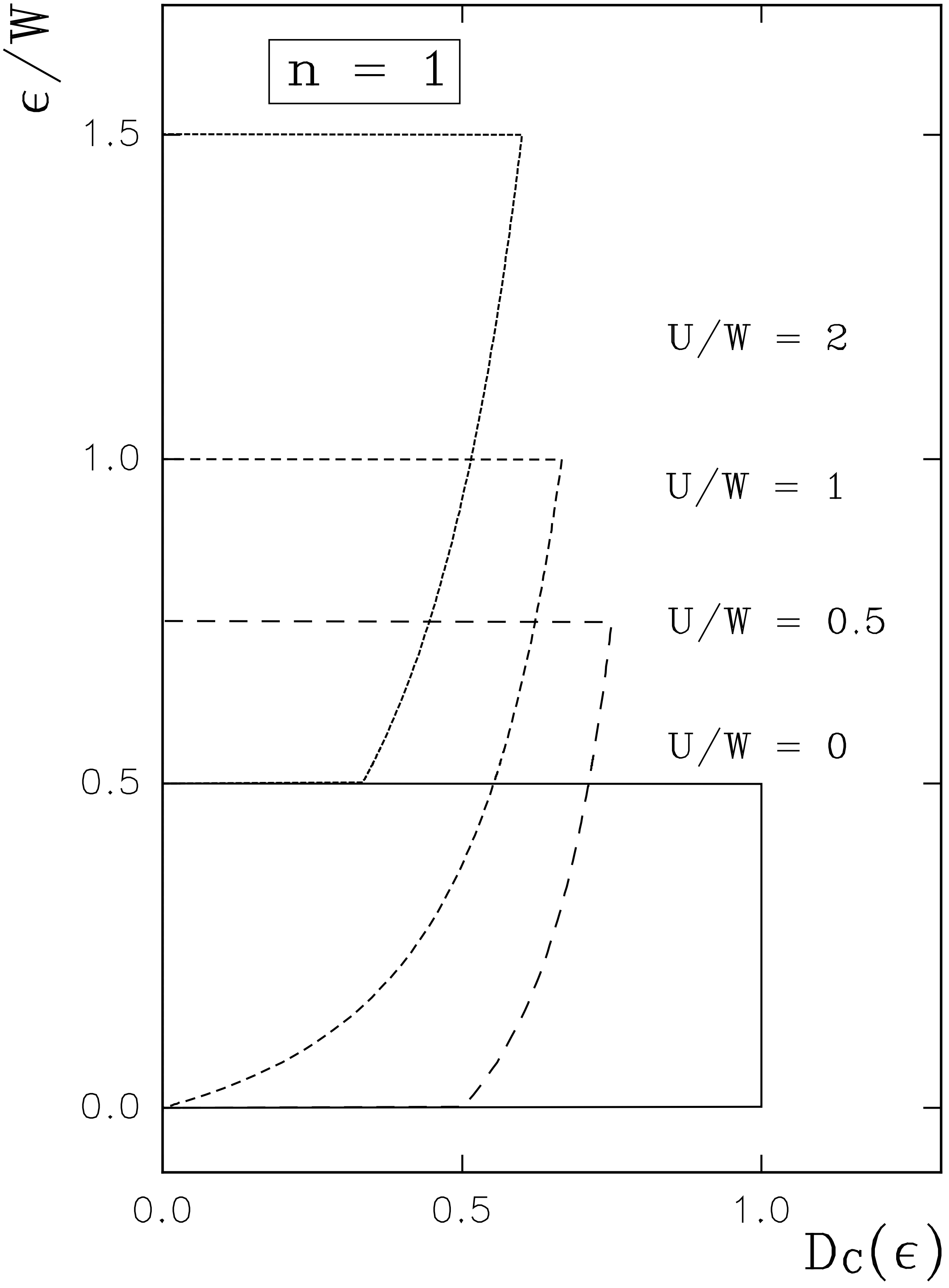
ε/W
n = 1
1.5
1.0
0.5
0.0
U/W = 2
U/W = 1
U/W = 0.5
U/W = 0
0.0
0.5
1.0
Dc(ε)

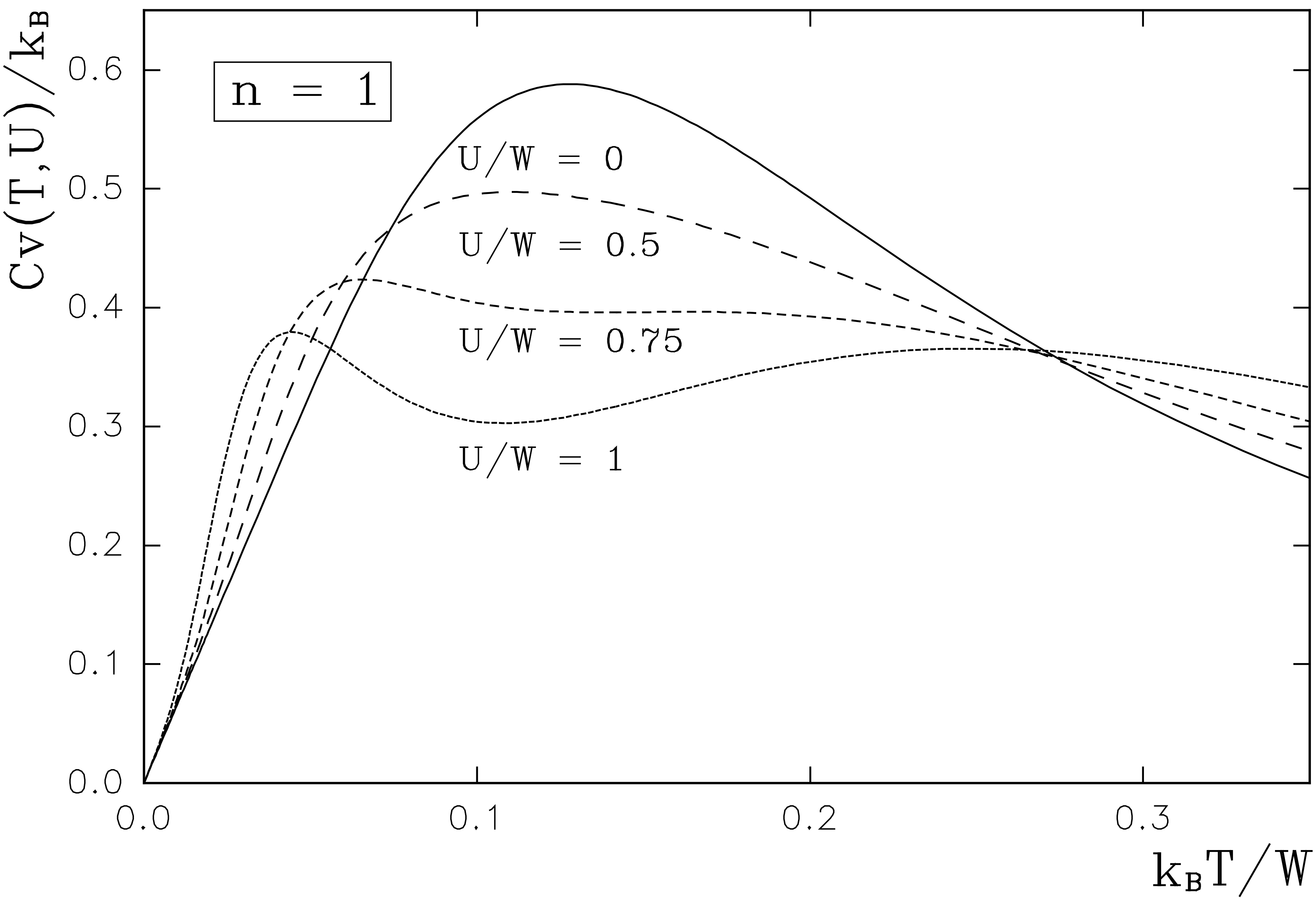

Cv(T,U)/k_B
n = 1
U/W = 0
U/W = 0.5
U/W = 0.75
U/W = 1
0.0
0.1
0.2
0.3
0.4
0.5
0.6
0.0
0.1
0.2
0.3
k_BT/W

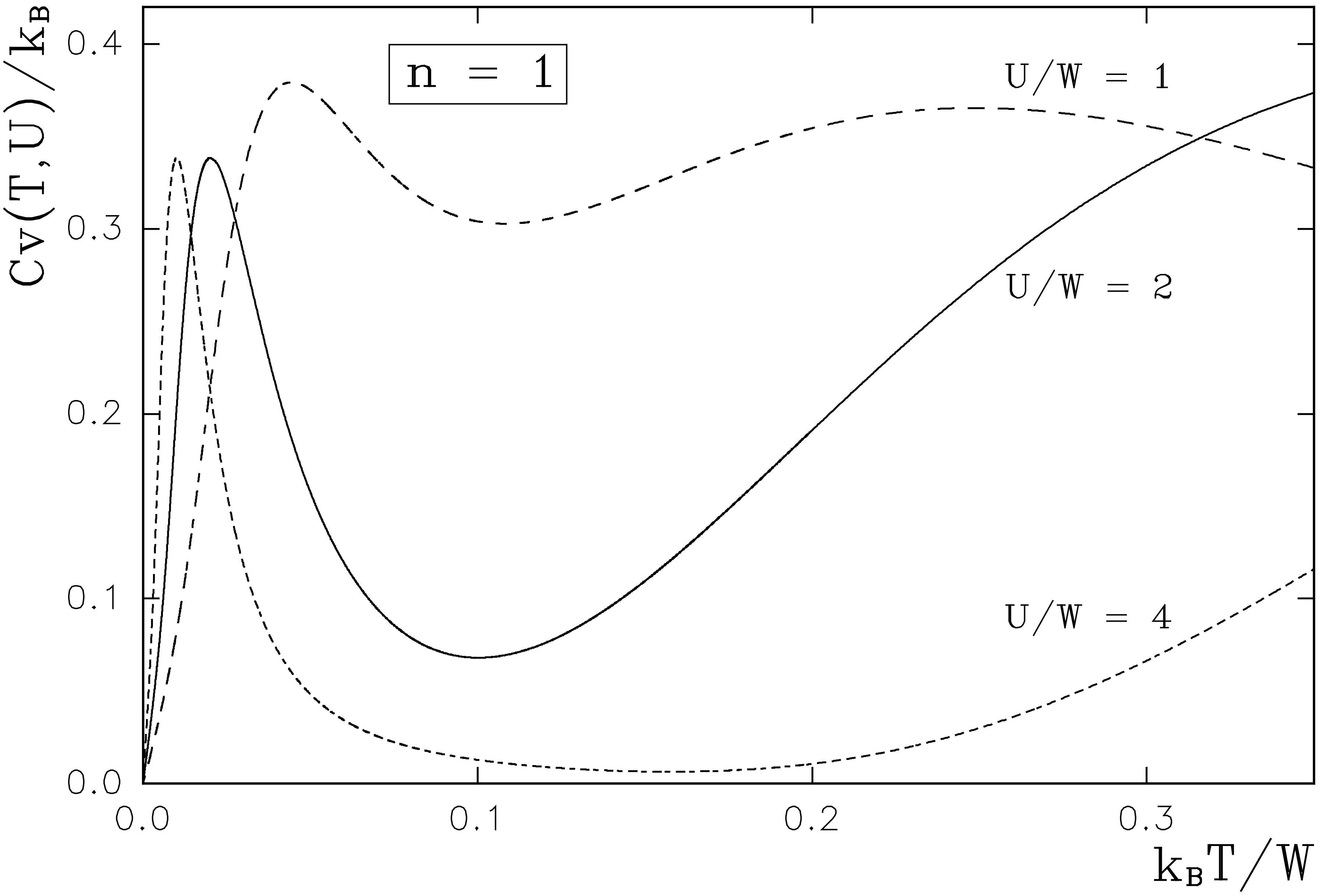
$C_V(T,U)/k_B$
0.4
0.3
0.2
0.1
0.0
n = 1
U/W = 1
U/W = 2
U/W = 4
0.0
0.1
0.2
0.3
k_BT/W

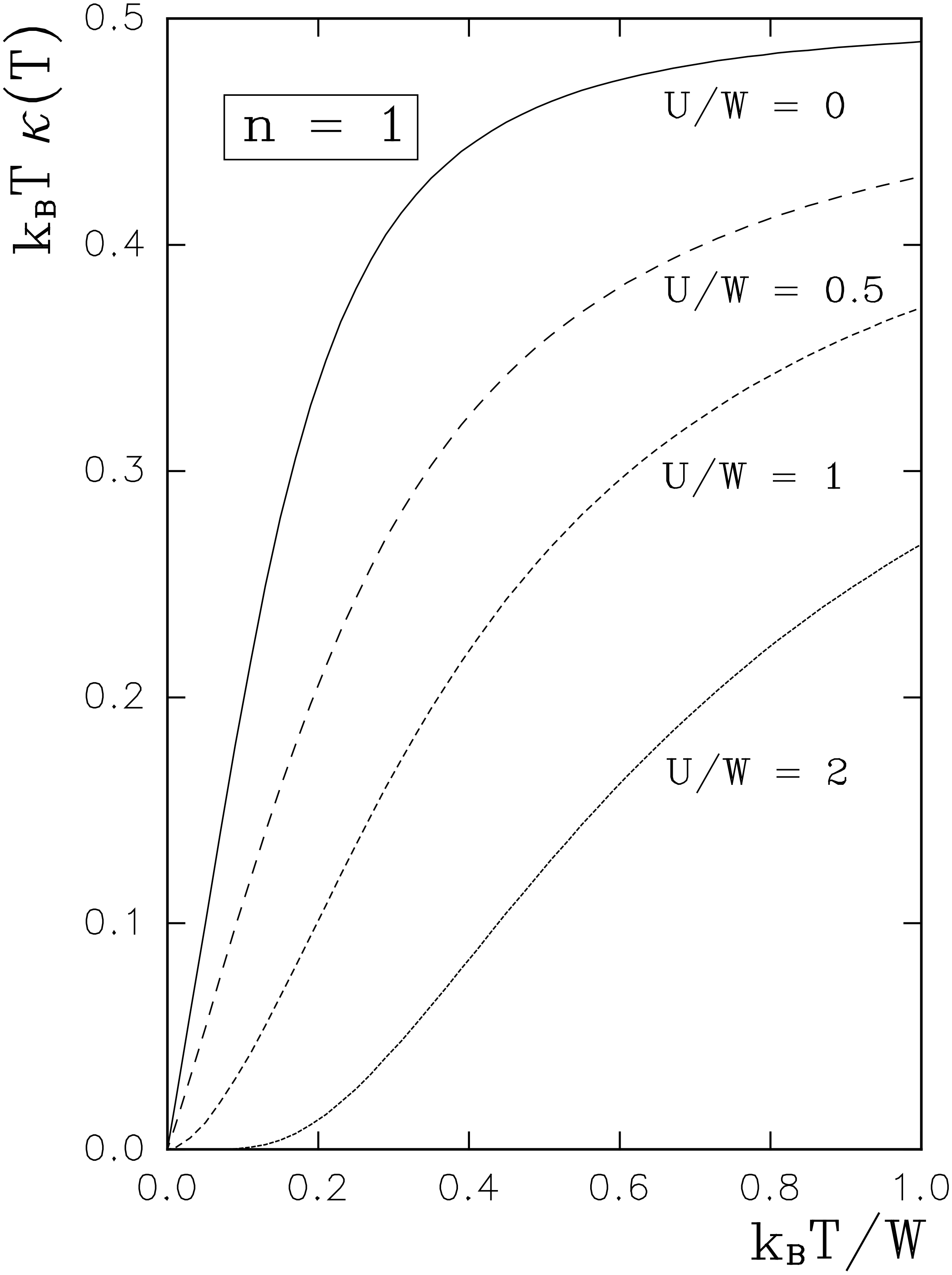

$k_B T\, \kappa(T)$
0.5
0.4
0.3
0.2
0.1
0.0
n = 1
U/W = 0
U/W = 0.5
U/W = 1
U/W = 2
0.0
0.2
0.4
0.6
0.8
1.0
$k_B T/W$

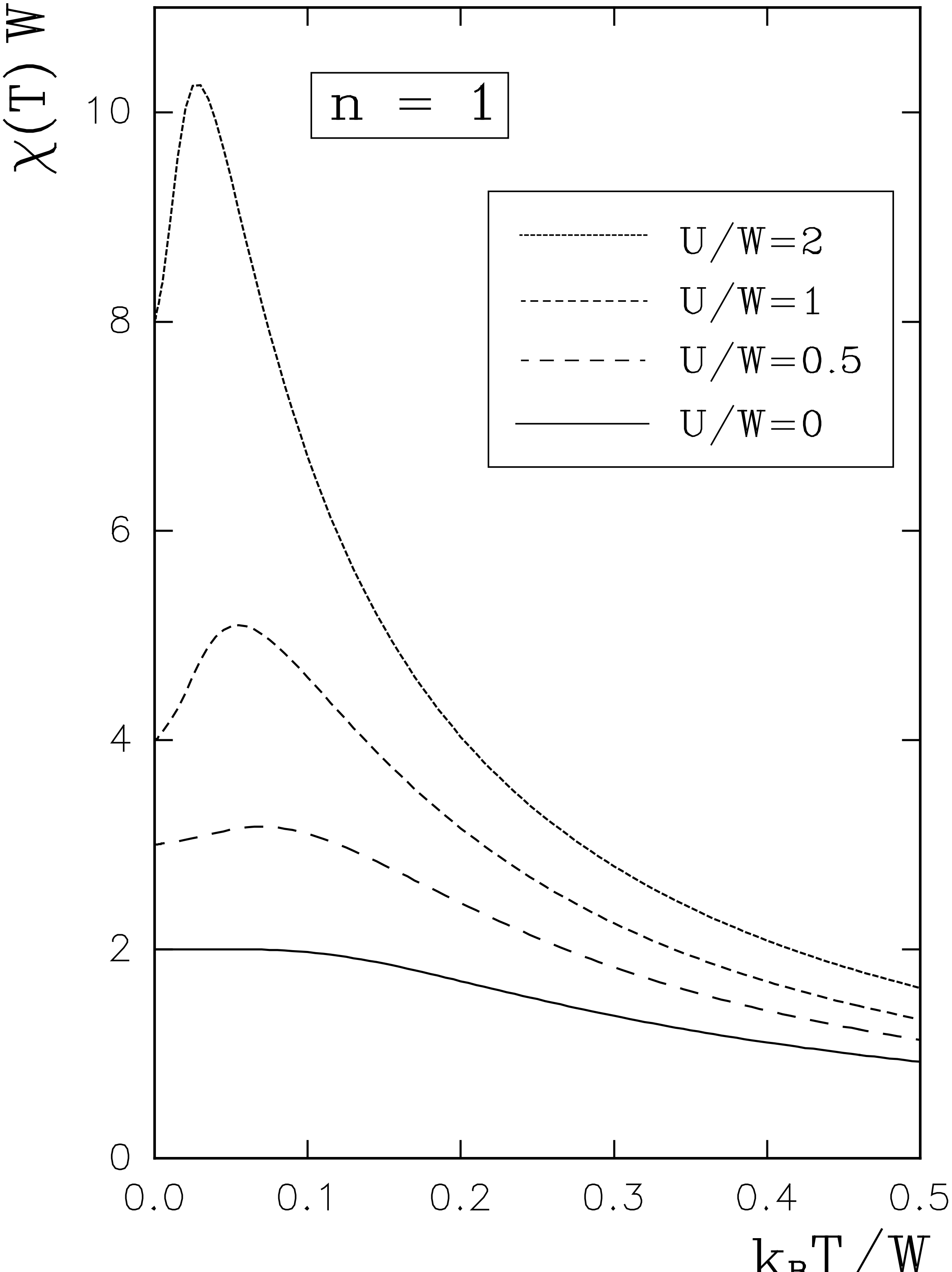

χ(T) W
n = 1
U/W=2
U/W=1
U/W=0.5
U/W=0
0
2
4
6
8
10
0.0
0.1
0.2
0.3
0.4
0.5
$k_B T/W$

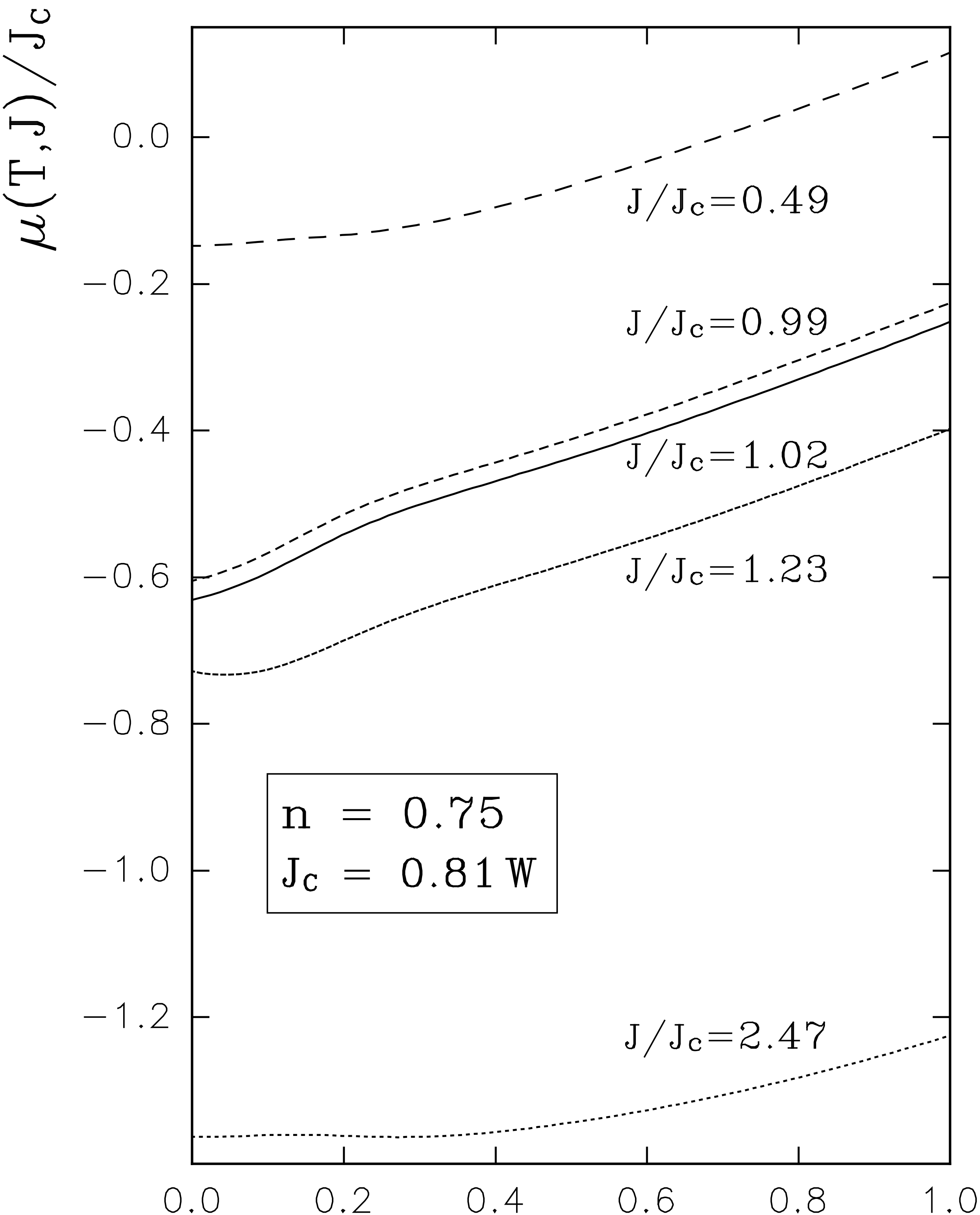

$\mu(T,J)/J_c$
0.0
−0.2
−0.4
−0.6
−0.8
−1.0
−1.2
0.0
0.2
0.4
0.6
0.8
1.0
$k_B T/J_c$
$J/J_c=0.49$
$J/J_c=0.99$
$J/J_c=1.02$
$J/J_c=1.23$
$J/J_c=2.47$
n = 0.75
J_c = 0.81 W

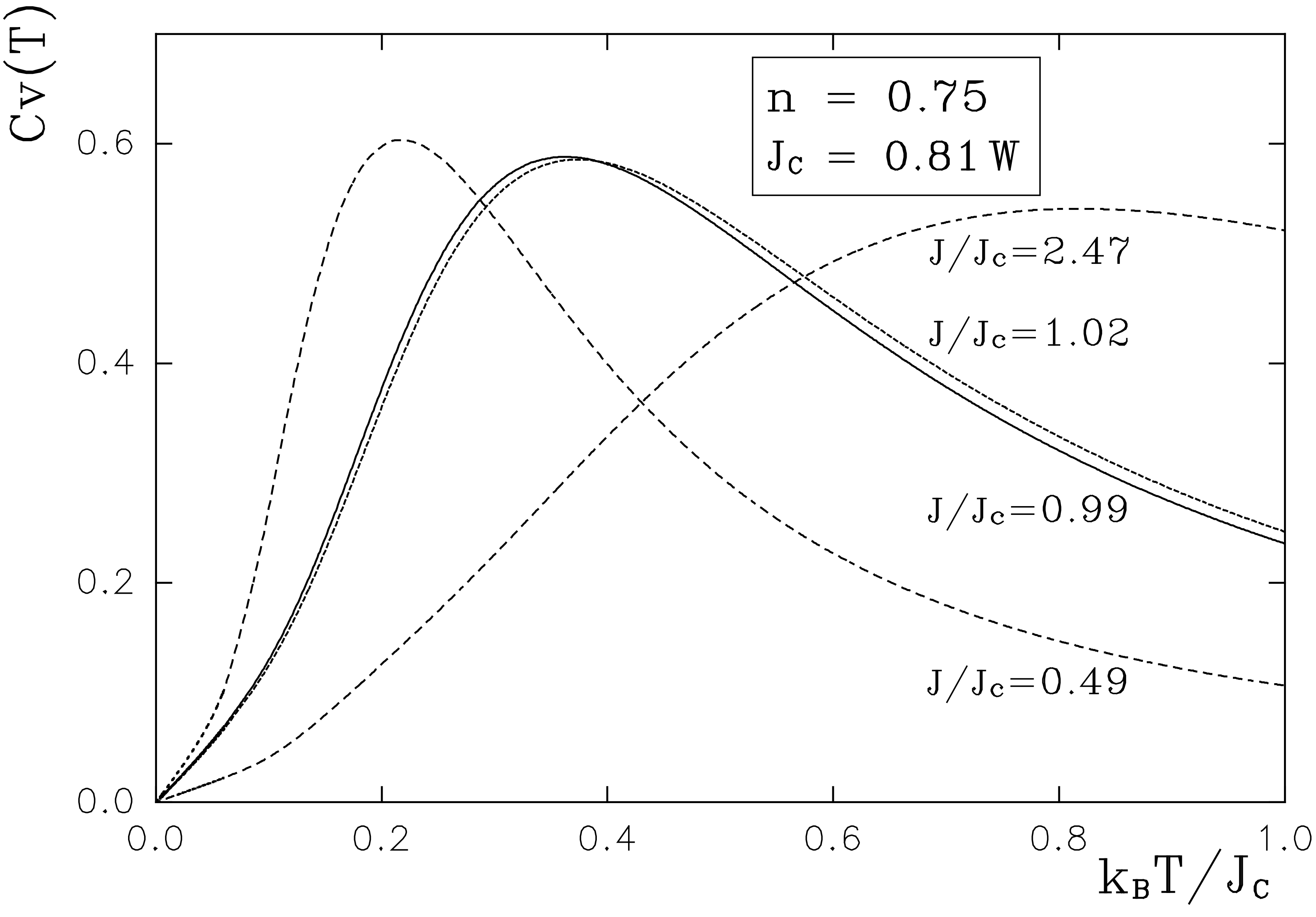
Cv(T)
n = 0.75
J_c = 0.81 W
J/J_c=2.47
J/J_c=1.02
J/J_c=0.99
J/J_c=0.49
0.0
0.2
0.4
0.6
0.0
0.2
0.4
0.6
0.8
1.0
$k_B T/J_c$

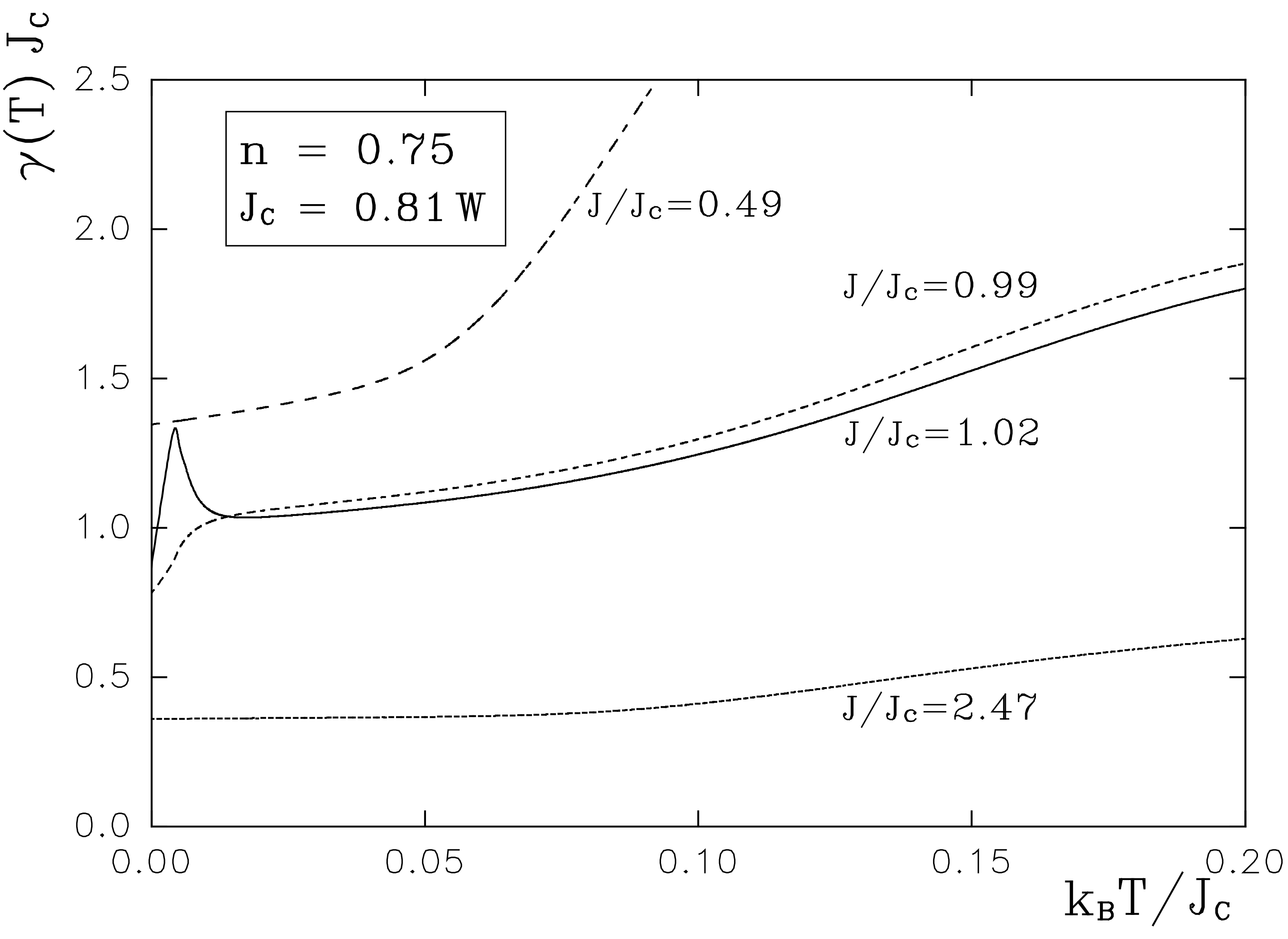

$\gamma(T)\,J_c$
2.5
2.0
1.5
1.0
0.5
0.0
n = 0.75
J_c = 0.81 W
J/J_c=0.49
J/J_c=0.99
J/J_c=1.02
J/J_c=2.47
0.00
0.05
0.10
0.15
0.20
k_BT/J_c

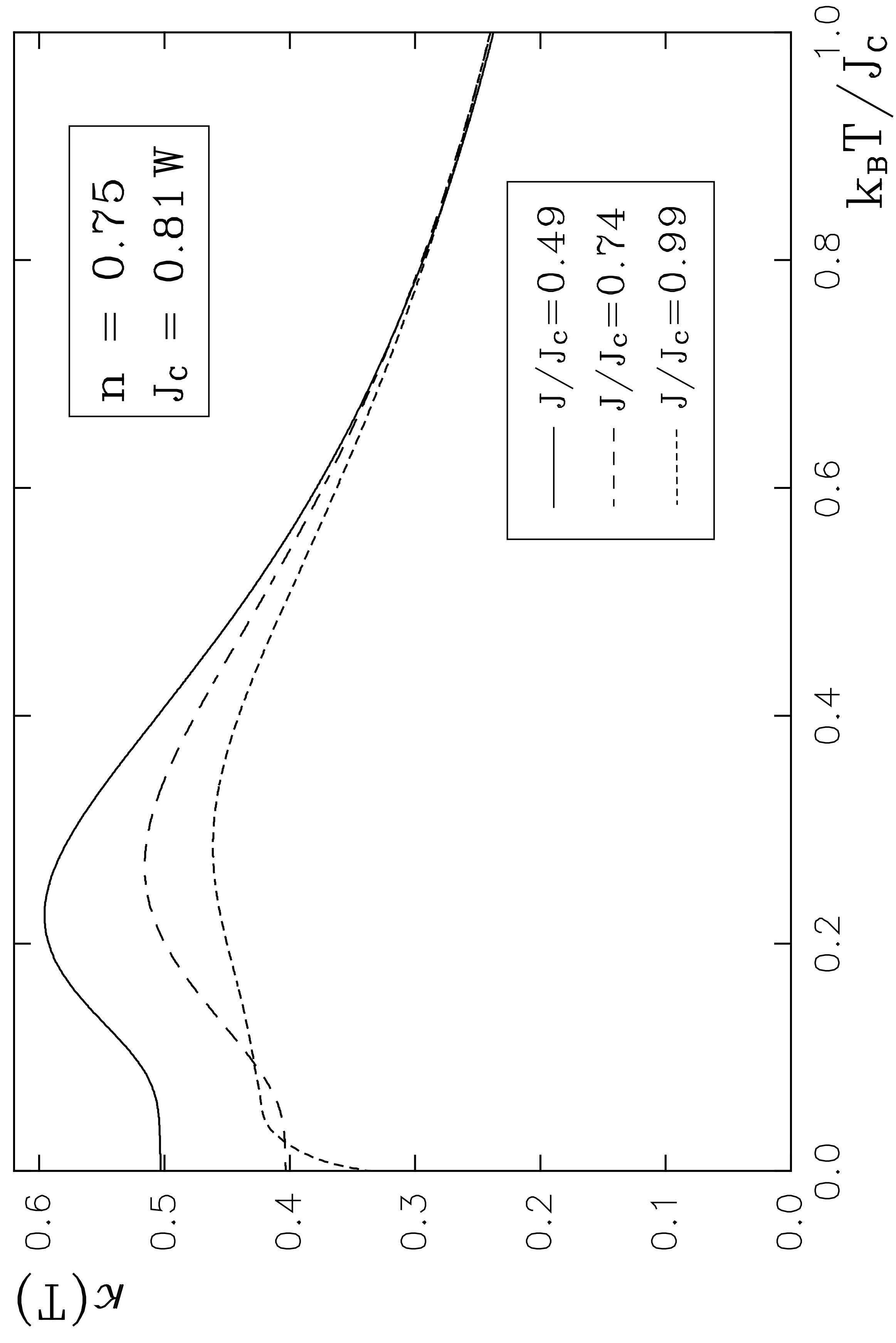

n = 0.75
J_c = 0.81 W
J/J_c=0.49
J/J_c=0.74
J/J_c=0.99
κ(T)
0.0
0.1
0.2
0.3
0.4
0.5
0.6
0.0
0.2
0.4
0.6
0.8
1.0
k_BT/J_c

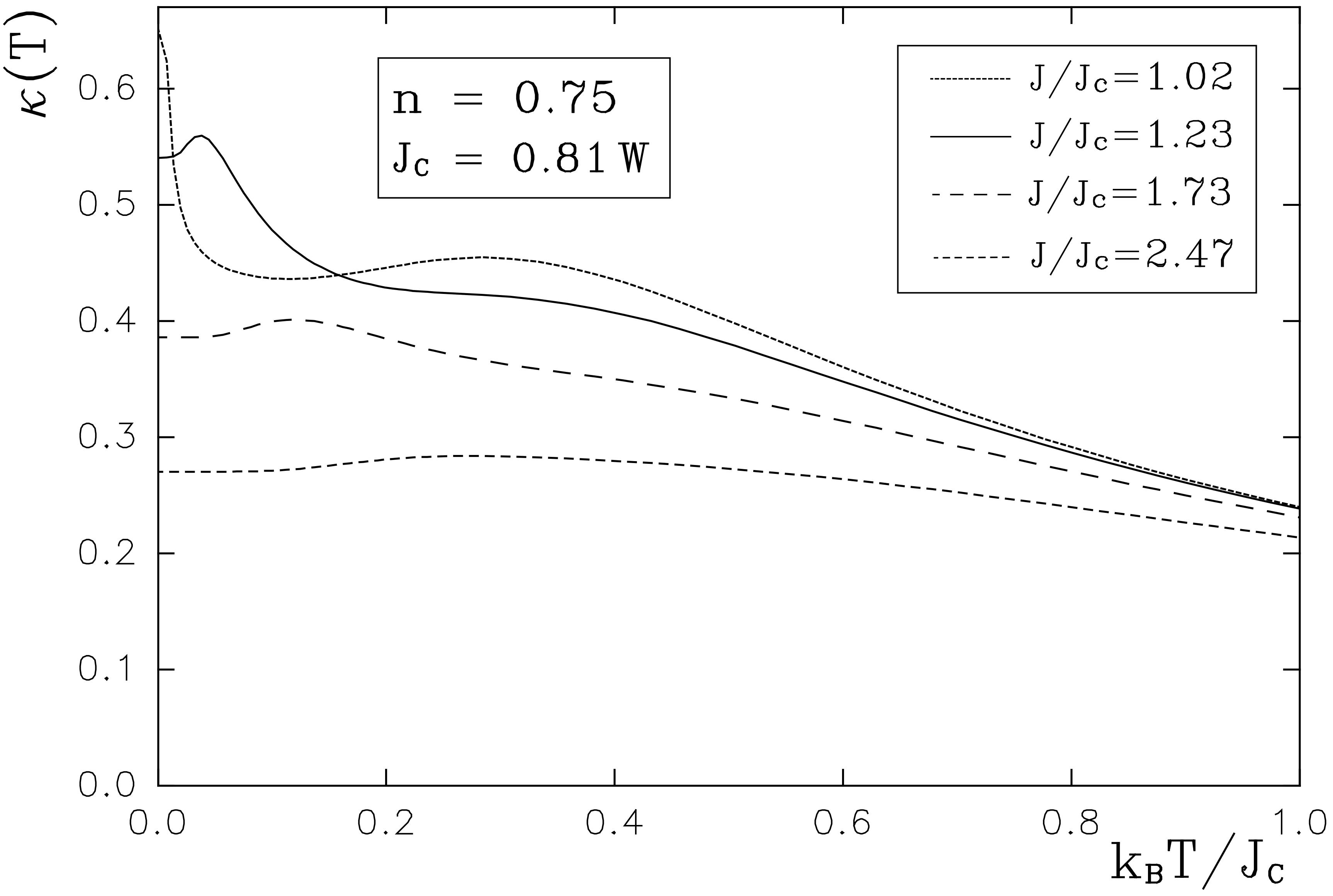
$\kappa(T)$
0.0
0.1
0.2
0.3
0.4
0.5
0.6
0.0
0.2
0.4
0.6
0.8
1.0
$k_B T/J_c$
$n = 0.75$
$J_c = 0.81\,W$
$J/J_c=1.02$
$J/J_c=1.23$
$J/J_c=1.73$
$J/J_c=2.47$

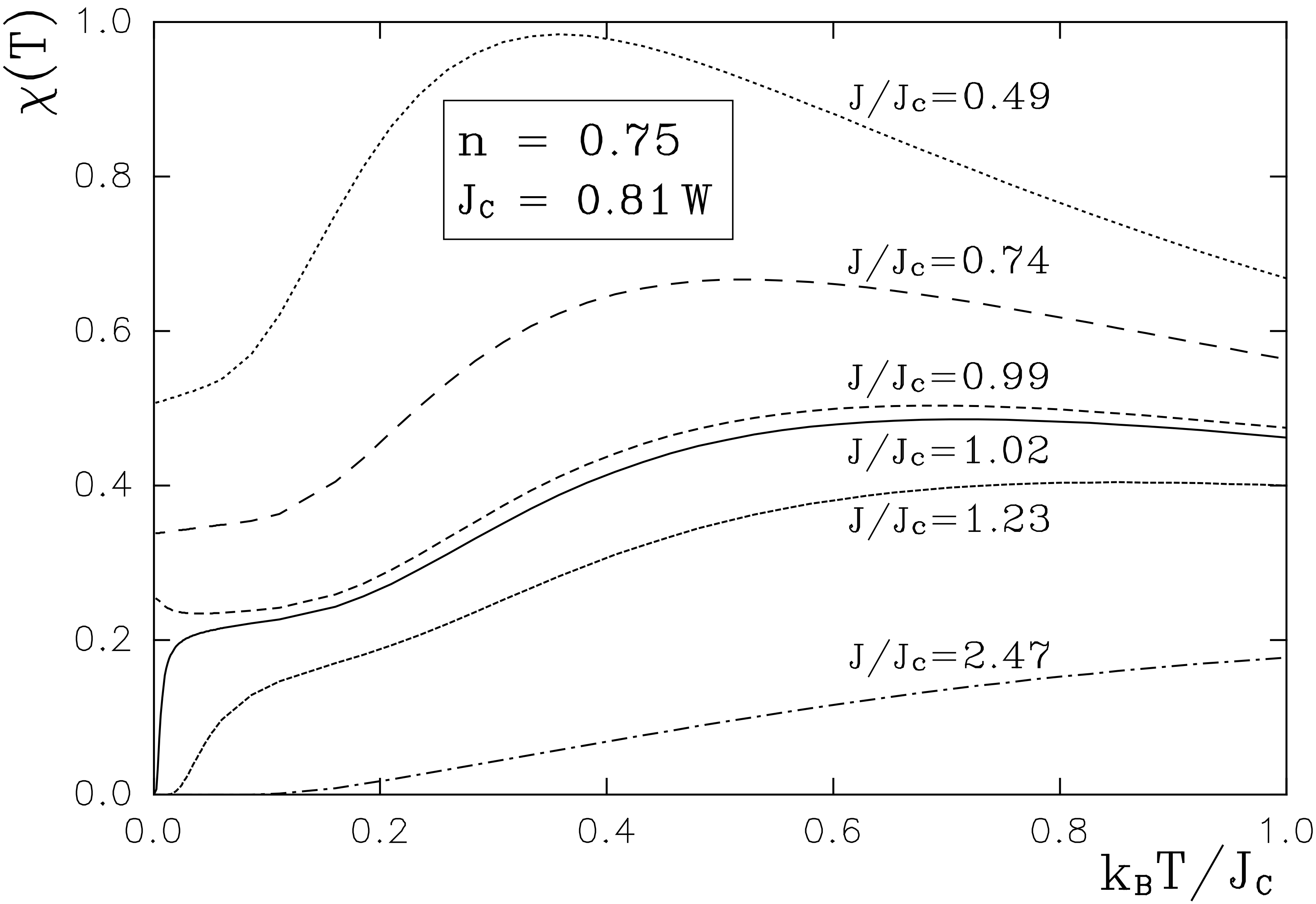
χ(T)
1.0
0.8
0.6
0.4
0.2
0.0
0.0
0.2
0.4
0.6
0.8
1.0
$k_B T/J_c$
n = 0.75
J_c = 0.81 W
J/J_c=0.49
J/J_c=0.74
J/J_c=0.99
J/J_c=1.02
J/J_c=1.23
J/J_c=2.47